Received: 30 November 2020 | Revised: 28 December 2020 | Accepted: 6 January 2021

DOI: 10.1002/eom2.12084

EcoMat FUNCTIONAL MATERIALS FOR GREEN ENERGY AND ENVIRONMENT WILEY

REVIEW

Strategy for large-scale monolithic Perovskite/Silicon tandem solar cell: A review of recent progress

Chan Ul Kim | Eui Dae Jung | Young Wook Noh | Seong Kuk Seo | Yunseong Choi | Hyesung Park | Myoung Hoon Song | Kyoung Jin Choi

Department of Materials Science and Engineering, Ulsan National Institute of Science and Technology (UNIST), Ulsan, Republic of Korea

Correspondence
Myoung Hoon Song and Kyoung Jin Choi, Department of Materials Science and Engineering, Ulsan National Institute of Science and Technology (UNIST), UNIST-gil 50, Ulsan 44919, Republic of Korea.
Email: mhsong@unist.ac.kr (M. H. S.) and choi@unist.ac.kr (K. J. C.)

Funding information
KOREA East-West Power Co., LTD. (EWP), Grant/Award Number: 2.190433.01; Korea Institute of Energy Technology Evaluation and Planning, Grant/Award Numbers: 20163010012450, 20193091010460; National Research Foundation of Korea, Grant/Award Number: 2019M1A2A2072416

Abstract

For any solar cell technology to reach the final mass-production/commercialization stage, it must meet all technological, economic, and social criteria such as high efficiency, large-area scalability, long-term stability, price competitiveness, and environmental friendliness of constituent materials. Until now, various solar cell technologies have been proposed and investigated, but only crystalline silicon, CdTe, and CIGS technologies have overcome the threshold of mass-production/commercialization. Recently, a perovskite/silicon (PVK/Si) tandem solar cell technology with high efficiency of 29.1% has been reported, which exceeds the theoretical limit of single-junction solar cells as well as the efficiency of stand-alone silicon or perovskite solar cells. The International Technology Roadmap for Photovoltaics (ITRPV) predicts that silicon-based tandem solar cells will account for about 5% market share in 2029 and among various candidates, the combination of silicon and perovskite is the most likely scenario. Here, we classify and review the PVK/Si tandem solar cell technology in terms of homo- and hetero-junction silicon solar cells, the doping type of the bottom silicon cell, and the corresponding so-called normal and inverted structure of the top perovskite cell, along with mechanical and monolithic tandemization schemes. In particular, we review and discuss the recent advances in manufacturing top perovskite cells using solution and vacuum deposition technology for large-area scalability and specific issues of recombination layers and top transparent electrodes for large-area PVK/Si tandem solar cells, which are indispensable for the final commercialization of tandem solar cells.

KEYWORDS

large scale, monolithic, PVK/Si, tandem solar cell

1 | INTRODUCTION

Crystalline silicon solar cells account for more than 95% of the total market share, and the remaining 5% is from CIGS- and CdTe-based solar cells.[1] In order for a specific solar cell technology to reach the final commercialization stage, it must satisfy not only the technical criteria, such as high efficiency,[2] long-term stability,[3] and the

possibility of a large area,[4] but also the socio-economic criteria such as price competitiveness,[5] human body, and environmental friendliness[6] of constituent materials. A wide variety of solar cell concepts have been proposed, and intensive research has been conducted to satisfy the above-mentioned criteria till now, but most of these technologies have not exceeded the threshold of final mass production commercialization.

Currently, the cost of crystalline silicon solar cells represented by Al-BSF or PERC has already fallen below 10 cents per watt and is predicted to decrease continuously to ~7 cents by reducing the amount of polysilicon used, as the wafer thickness decreases or the increase in power generation per cell as the wafer size increases from M2 to M12.[7] Therefore, there is no doubt that crystalline silicon solar cells will maintain the best price competitiveness among all solar cell technologies in the future, but the efficiency is already approaching the practical limiting efficiency of single-junction solar cells, requiring an innovative strategy.[8] A multi-junction or tandem solar cell manufactured by stacking a semiconductor PN junction with a large bandgap on top of another semiconductor PN junction with a small bandgap is one of the alternatives that can overcome the fundamental efficiency limitations of a silicon solar cell.[9] The III to V compound semiconductor-based triple tandem solar cell was recognized as one of the ultra-high-efficiency solar cell candidates with high efficiency of 37.9%.[10] However, III to V compound semiconductor technology has failed to commercialize mass production because it requires expensive vacuum equipment and precursors for thin-film synthesis and is known to be harmful to the human body and environment.[11,12] As an alternative, studies on implementing tandem solar cells of various structures by stacking various low-cost solar cells have been intensively studied in recent years. Top cell candidates include organic solar cells,[13] CIGS solar cells, dye-sensitized solar cells,[14] and perovskite (PVK) solar cells[15] with relatively high bandgap energy, while bottom cells include narrow bandgap materials such as silicon solar cells and CIGS.[16] Representative heterojunction tandem solar cells are as follows: Dye-sensitized solar cells/silicon tandem solar cells using PEDOT:FTS with higher transparency and lower charge transfer resistance than Pt used as an interfacial catalyst layer,[14] solution-processed organic/organic tandem solar cells guided by a semi-empirical analysis,[17] PVK/CIGS tandem solar cells with conformal monolayer contacts with lossless interfaces,[18] PVK/organic tandem solar cells with low-loss interconnecting layers,[19] a monolithic all-PVK tandem solar cell with a strategy to reduce Sn vacancies in mixed Pb-Sn narrow-bandgap PVKs[20] have been reported.

Among these various heterogeneous tandem solar cell technologies, perovskite/silicon (PVK/Si) tandem solar cells are considered to have the highest potential in terms of high efficiency and price competitiveness. The German research team reported a PVK/Si tandem solar cell with an efficiency of 29.1%, which exceeds the theoretical limit of a single junction solar cell close to a standalone silicon or PVK solar cell.[21] Comprehensive optical simulations conducted by various research institutes show that when the current matching of the monolithic PVK/Si tandem solar cell is optimized, the ideal current density value is ~21 mA/cm^2, and the corresponding efficiency is reported to be ~31%.[22-24] In order to achieve such an ideal current density, novel device structures, and new materials that can minimize light reflection at the surface and parasitic light absorption by electron and hole transport layers need to be designed. Because silicon solar cells are known to be very stable devices, the long-term stability issue of PVK/Si tandem solar cells stems entirely from top PVK cells.[25] Recently, through intensive research on the improvement of long-term stability of PVK solar cells, it was found that forming A and X sites in a mixed composition rather than a single composition greatly improves the stability of the solar cell.[26,27] More stable PVK thin films with minimal lattice mismatch can be formed through mixed-cation and mixed-halide approaches designed in consideration of a tolerance factor.[28] In this review article, we have categorized and discussed the differences, advantages, and disadvantages of tandem solar cells depending on the type of doping or junction of bottom silicon solar cells. In particular, we review the recent advances in manufacturing top PVK cells using solution and vacuum deposition technology for large-area scalability along with specific issues of recombination layers and top transparent electrodes for large-area PVK/Si tandem solar cells, which are indispensable for the final commercialization of tandem solar cells.

2 | CLASSIFICATION OF PVK/Si TANDEM SOLAR CELLS IN TERMS OF STRUCTURE TYPES

2.1 | The 4-terminal PVK/Si tandem solar cell

The 4-terminal (4T) tandem solar cells have the advantage that the top and bottom cells can independently contribute to the maximum output power because the top and bottom cells are only optically coupled without electrical connection by using the top solar cells as filters. (Figure 1B,C). In order to maximize the efficiency of a 4T tandem solar cell, it is necessary to maximize the efficiency of each top and bottom cell at the matching point of current and voltage, respectively. The highest theoretical 4T tandem solar cell has a PCE of 46% (Figure 1E).[15]

Taking advantage of these 4T tandem solar cells, various 4T tandem solar cells are being studied. Si solar cells, which occupy the mainstream of the solar cell market, are the most suitable candidates for commercialization in tandem solar cell research.[29] In addition, PVK with a tunable bandgap is a suitable candidate as the top cell of a Si-based tandem solar cell.[30] The structure of a typical 4T tandem PVK/Si solar cell can be classified as follows. There are PIN structured PVK top cell/n-si based homojunction Si bottom cell (Figure 2A),[31] NIP structured PVK top cell/p-si based homojunction Si bottom cell (Figure 2B),[32] PIN structured PVK top cell/n-si based heterojunction Si bottom cell (Figure 2C)[31] and NIP structured PVK top cell/n-si based heterojunction Si bottom cell (Figure 2D).[33]

Representative 4T PVK/Si tandem solar cells based on a homojunction Si bottom cell as a function of the type of top cell structures such as NIP or PIN. Bailie et al developed the first 4T PVK/Si tandem solar cells with 17% efficiency by using a silver nanowire transparent electrode on an NIP structure PVK top cell based on $CH_3NH_3PbI_3$ and applied it to a low-quality multi-crystalline Si bottom cell.[16] Duong et al analyzed the electrical and optical power loss in detail and produced an NIP structured PVK top cell of >80% near-infrared transmittance based on the design for the optimal tandem cell with ITO transparent electrode.[34] This was applied to the PERL cell, and an efficiency of 20.1% was reported. Ren et al increased the efficiency of the NIP structured PVK top cell by using a PVK film with a low density of bandgap states applied with postdeposition oxygen treatment and developed a highly transparent $MoO_3/Au/MoO_3$ electrode.[35] This was applied on a p-Si-based homojunction Si bottom cell to fabricate a 4T tandem solar cell and reported efficiency of 23.6%. Ren et al obtained high transmittance in the long-wavelength range using a $MoO_3/Au/MoO_3$ transparent electrode.[36] An NIP structured $CH_3NH_3PbI_3$-based PVK top cell was fabricated by introducing a PVK thin film with reduced defect density using oxygen annealing treatment. In addition, a novel bio-mimicking elastomeric

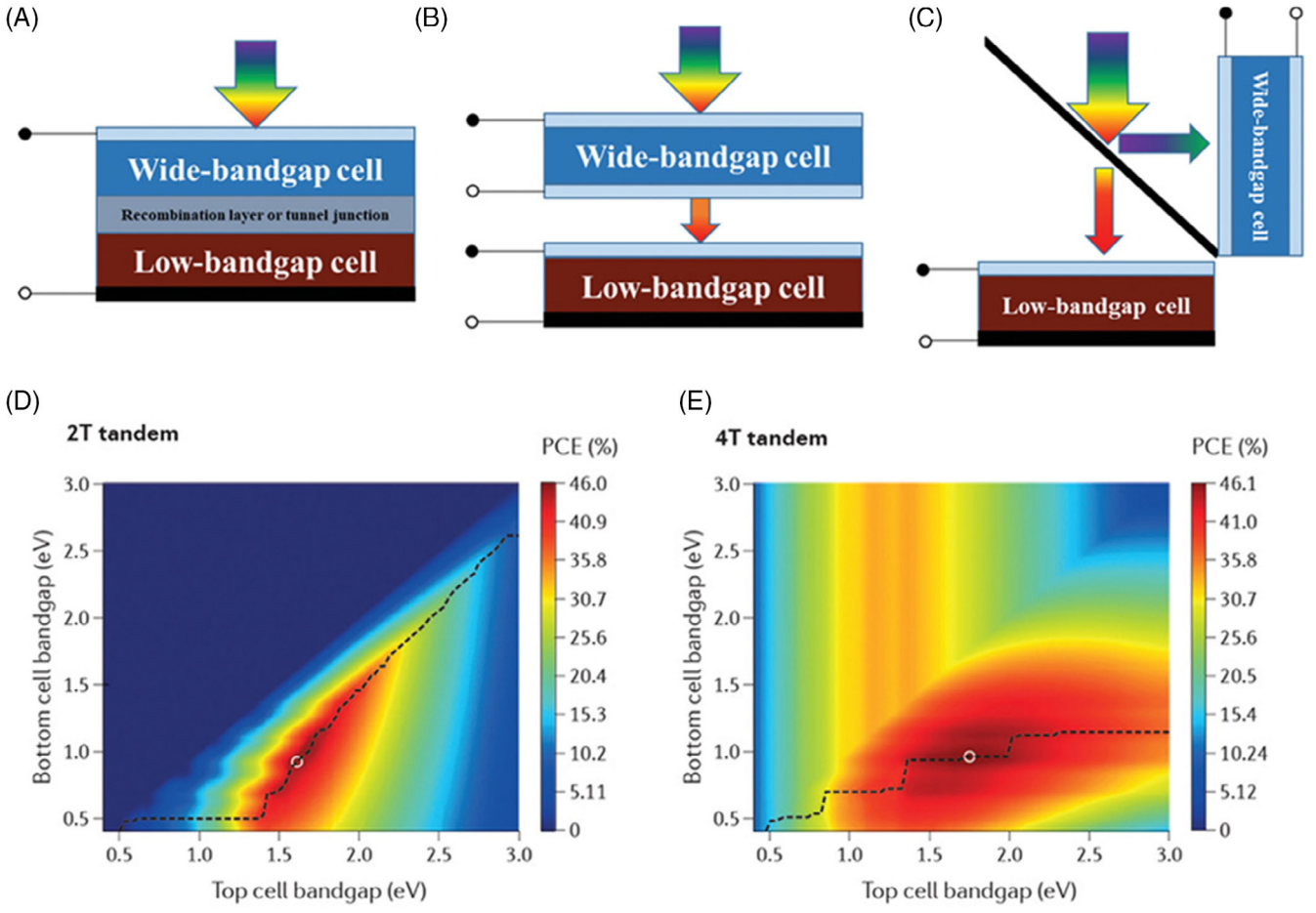

FIGURE 1 Schematics of tandem architectures: (A) 4-terminal mechanically stacked (B) 2-terminal monolithically integrated (C) 4-terminal optical spectral splitting. (D) and (E) theoretical maximum PCE for 2T and 4T tandem solar cells. Reproduced with permission: Copyright 2019, John Wiley and Sons[15]

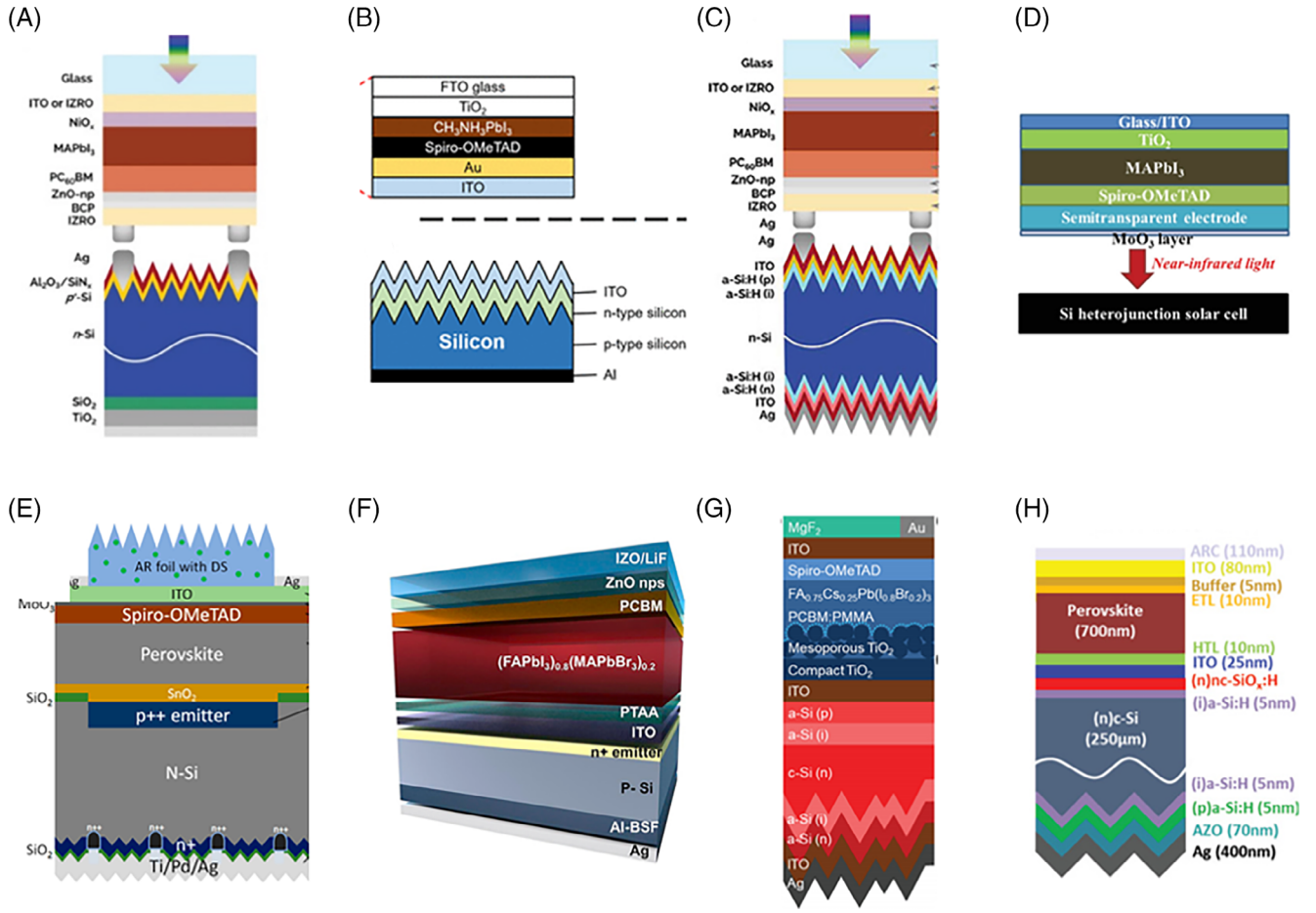

FIGURE 2 Schematics of PVK/Si tandem architectures: 4-terminal mechanically stacked (A) PIN structured PVK top cell/n-si based homojunction Si bottom cell. Reproduced with permission: Copyright 2019, John Wiley and Sons.[31] (B) NIP structured PVK top cell/p-si based homojunction Si bottom cell. Copyright 2019 American Chemical Society.[32] (C) PIN structured PVK top cell/n-si based heterojunction Si bottom cell. Reproduced with permission: Copyright 2019, John Wiley and Sons.[31] (D) NIP structured PVK top cell/n-si based heterojunction Si bottom cell, 2-terminal monolithically integrated. Reproduced with permission: Copyright 2019, John Wiley and Sons.[33] (E) NIP structured PVK top cell/n-si based homojunction Si bottom cell. Copyright 2019 American Chemical Society.[53] (F) PIN structured PVK top cell/p-si based homojunction Si bottom cell. Copyright 2019 Elsevier Ltd.[54] (G) NIP structured PVK top cell/n-si based heterojunction Si bottom cell. Reproduced with permission: Copyright 2019, John Wiley and Sons.[55] (H) PIN structured PVK top cell/n-si based heterojunction Si bottom cell Reproduced with permission: Copyright 2019, John Wiley and Sons[56]

petal-based light trapping layer was developed and applied to the top cell and introduced on the PERC to make a 4T PVK/Si tandem solar cell and reported efficiency of 22.4%. Dewi et al compared mesoporous TiO_2 and planar SnO_2 that are used as electron transport layer (ETL) layers in an NIP structured PVK top cell.[37] By applying these ETLs, the PVK top cells based on $Cs_{0.05}(MA_{0.17}FA_{0.83})_{0.95}Pb(I_{0.83}Br_{0.17})_3$) and ($FA_{0.83}Cs_{0.17}PbI_2Br$) with 1.58 and 1.72 eV band gaps were produced. This top cell was applied to an n-Si-based homojunction Si bottom cell to make a 4T PVK/Si tandem solar cell and reported efficiencies of 25.5% (1.58 eV) and 22.4% (1.72 eV). Najafi et al developed an PIN structured PVK top cell with ZnO ETL as a sputtering damage buffer layer by employing the ALD process.[38] This top cell was applied to the PERT cell to make a 4T tandem solar cell and reported efficiency of 21.1%. Quiroz et al developed an all-solution PVK solar cell to improve the transmittance in the infrared wavelength range and introduced CuSCN as the anti-reflection coating (ARC) layer and used it as a selective contact between the transparent electrode and the PVK.[39] A silver nanowire electrode with a transmittance of 84% or more in the region of 300 to 1100 nm was introduced into the top cell of $CH_3NH_3PbI_3$-based PVK having an PIN structure. This was applied to the bottom cell of each of the PERL cells to make a 4T PVK/Si tandem solar cell and reported an efficiency of 26.7%. Duong et al fabricated a PVK top cell of $Rb_{0.05}Cs_{0.095}MA_{0.1425}FA_{0.7125}PbI_2Br$ with a band gap of 1.72 eV.[40] In addition, the 2D PVK precursor as MABr

was introduced on the 3D PVK film, and this result showed that the device performance was improved by reducing the surface defects of the 3D PVK film. This top cell was placed on the PERL cell to make a 4T PVK/Si tandem solar cell, and an efficiency of 26.2% (1 cm^2) was reported.

As representative 4T PVK/Si tandem solar cells of NIP structured PVK top cell or PIN structured PVK top cell based on heterojunction Si bottom cell, for the first time, Löper et al obtained a transmittance of >55% in the near-infrared spectral region by using an ITO transparent electrode design without a metallic component on a PVK top cell with an NIP structure based on $CH_3NH_3PbI_3$.[41] This technology was applied to a heterojunction Si bottom cell to make a 4T PVK/Si tandem solar cell, and due to high transmittance, the current density value of the bottom cell was increased, and an efficiency of 13.4% was reported. Werner et al used a MoO_x buffer layer to protect sputtering damage and used an indium zinc oxide (IZO) layer having an absorption of less than 3% at 400 to 1200 nm and sheet resistance of 35 Ω/sq as a transparent electrode.[42] The $CH_3NH_3PbI_3$-based PVK top cell of the NIP structure using this transparent electrode obtained >60% transmittance in the 800 to 1200 nm wavelength range. This top cell was applied on a heterojunction Si bottom cell to increase the current density to make a 4T PVK/Si tandem solar cell with an efficiency of 18.18%. Werner et al fabricated a $CH_3NH_3PbI_3$-based PVK top cell with an NIP structure that increased the area from 0.2 to 1 cm^2.[43] This was applied to a heterojunction Si solar cell on top to make a 4T PVK/Si tandem solar cell and reported efficiencies of 23.0% (1 cm^2) and 25.2% (0.25 cm^2). Yang et al fabricated an NIP structured PVK top cell based on $FA_{0.83}Cs_{0.17}Pb(I_{0.6}Br_{0.4})_3$ with a wide bandgap of 1.75 eV using nonstoichiometric precursor chemistry with excess methylammonium halides and applied it to a heterojunction Si solar cell.[44] Thus, a 4T PVK/Si tandem solar cell was produced and an efficiency of 20.3% was reported. Zhang et al made a 4T PVK/Si tandem solar cell by introducing an PIN structure ($Cs_{0.05}(MA_{0.17}FA_{0.83})_{0.95}Pb(I_{0.9}Br_{0.1})_3$) based PVK top cell on the IBC cell with ~92% near-infrared transmittance[45] that reported efficiency of 25.7%. Jaysankar et al designed a 4T PVK/Si tandem solar cell structure with minimal light loss when the Si surface was textured and flat based on optical simulation.[46] Based on this design, a 4T PVK/Si tandem solar cell was fabricated by applying a PVK top cell based on the NIP structure of $Cs_{0.1}FA_{0.9}PbI_{2.865}Br_{0.135}$ on the IBC bottom cell to produce efficiencies of 25.5% (0.13 cm^2) and 23.9% (4 cm^2). Wang et al introduced an ultrathin gold nanomesh layer using the Frank-van der Merwe growth method to fabricate a MoO_x/Au/MoO_x transparent electrode.[33] An NIP structured $CH_3NH_3PbI_3$ based PVK top cell was introduced for this electrode, and a 4T PVK/Si tandem solar cell was fabricated by applying the top cell on the heterojunction Si bottom cell, and an efficiency of 27% was reported. Jaysankar et al introduced an Al_2O_3 passivation layer using an ALD process between the PVK layer based on $Cs_{0.15}(CH_5NH_2)_{0.85}Pb(I_{0.71}Br_{0.29})_3$ and the spiro layer used as hole transport layer (HTL).[47] By minimizing the nonradiative recombination of the PVK top cell with a 1.72 eV bandgap, open-circuit voltage (V_{oc}) deficit was reduced, and a high V_{oc} value of 1.22 V was obtained. A 4T PVK/Si tandem solar cell was fabricated by applying the top cell with an Al_2O_3 passivation layer on top of the IBC bottom cell and reported efficiencies of 27.1% (0.13 cm^2) and 25.3% (4 cm^2). Aydin et al introduced a Zr-doped indium oxide (IZRO) transparent electrode, which has a better near-infrared response than the commercially used ITO.[31] This was applied to a $CH_3NH_3PbI_3$-based PVK top cell with an NIP structure and placed on a heterojunction Si bottom cell to make a 4T PVK/Si tandem solar cell and reported an efficiency of 26.2%. Gharibzadeh et al fabricated an NIP structured PVK top cell based on ($FA_{0.83}Cs_{0.17}Pb[I_{1-y}Br_y]_3$) with a bandgap of 1.65 eV $\leq E_g \leq$ 1.85 eV.[48] In addition, by introducing 2D/3D PVK hetero-structure passivation to the top cell, V_{oc} of about 45 mV was increased. This top cell was applied to the IBC bottom cell to make a 4T PVK/Si tandem solar cell and reported an efficiency of 25.7%. Rohatgi et al pointed out the existing high-cost heterojunction Si sub-cell and fabricated a tunnel oxide passivated contact (TOPCon) sub-cell, which has higher commercialization potential than the heterojunction Si cell.[49] A $Cs_{0.05}FA_{0.8}MA_{0.15}PbI_{2.55}Br_{0.45}$ based PVK top cell of PIN structure was placed on top of the TOPCon bottom cell to make a 4T PVK/Si tandem solar cell and reported an efficiency of 26.7%. Dewi et al compared the previously reported filtered-based measurement method with a size matching scheme using a mask and mentioned the importance of optimal measurement schemes.[50] In the case of 4T PVK/Si tandem solar cells measured by this analysis method the efficiencies, 24.7% and 23.5%, respectively, showed a difference of approximately 1%.

The analysis of the flow of 4T PVK/Si tandem solar cell research that has been carried out so far (Figure 3 and Table S1) shows that it has the advantage of simply applying it to the previously optimized Si solar cell by making a PVK top cell with excellent long-wavelength transmittance. However, there is an air gap in the path where the light source passes through the PVK top cell and is transmitted to the Si bottom cell. This air gap causes a difference in refractive index between the PVK top cell and the Si bottom cell. In other words, optical loss

due to the difference in refractive index is a major cause of low efficiency. Therefore, in order to overcome the limitation of the efficiency of the 4T tandem solar cell, it is necessary to minimize the optical loss by reducing the parasitic absorption of each functional layer. In addition, there is a need for an interfacial layer technology capable of minimizing optical loss that can replace the air gap between the PVK top cell and the Si bottom cell.

2.2 | Monolithic 2-terminal PVK/Si tandem solar cell

The monolithic 2-terminal (2T) tandem solar cell has the advantage of less parasitic absorption, as it is a simple integrated type without additional glass substrate and thick transparent electrode for PVK top cell, but sophisticated technologies such as process optimization and current matching technology are required (Figure 1A).[15] Additionally, the cost of the glass substrate and thick transparent electrode of 4T tandem solar cells is also a drawback in commercialization compared to 2T tandem solar cells.[51] In order to maximize the efficiency of a 2T tandem solar cell, it is necessary to maximize the efficiency of each top and bottom cell at the matching point of current and voltage. The highest theoretical 2T tandem solar cell has a PCE of 45.7% (Figure 1D).[15] Among 2T tandem solar cells, the reason why PVK/Si tandem solar cell research is growing rapidly is that PVK thin films are easier to adjust the bandgap and thickness than other thin films.[52] That is, when a PVK thin film is applied as the top cell of a tandem device by using the specificity of such a PVK thin film, it is advantageous for the current matching of a tandem solar cell. To fabricate a 2T PVK/Si tandem solar cell, the polarity of the PVK top cell and Si bottom cell should be matched, and a semi-transparent PVK solar cell with high transparency in the near-infrared region should be fabricated directly on the Si bottom cell.[28] A typical 2T PVK/Si tandem solar cell design with a PVK top cell based on a Si solar cell is as follows. There are NIP structured PVK top cell/n-Si based homojunction Si bottom cell (Figure 2E),[53] PIN structured PVK top cell/p-Si based homojunction Si bottom cell (Figure 2F),[54] NIP structured PVK top cell/n-Si based heterojunction Si bottom cell (Figure 2G)[55] and PIN structured PVK top cell/n-Si based heterojunction Si bottom cell (Figure 2H).[56] As the advantages of Si and PVK solar cells, the following 2T PVK/Si tandem solar cells are rapidly being studied.

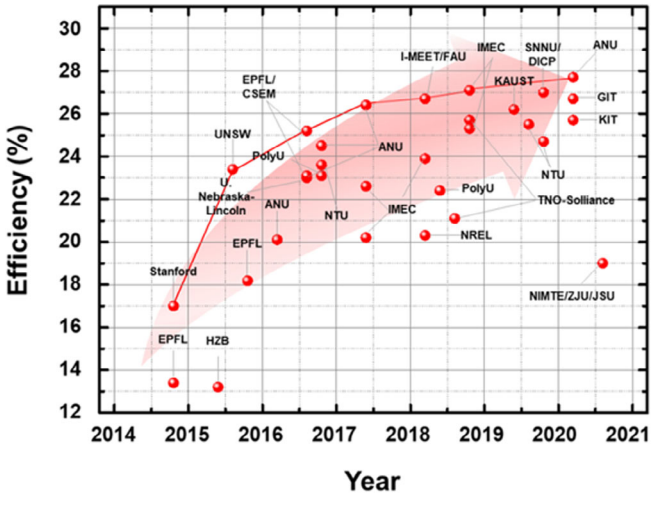

FIGURE 3 The efficiency chart of reported 4-terminal PVK/Si tandem solar cell

Representative 2T PVK/Si tandem solar cells based on an NIP structured PVK top cell and n-type homojunction Si bottom cell are described in this section. Mailoa et al[57] developed the first monolithic 2T PVK/Si tandem solar cell using an NIP structured $CH_3NH_3PbI_3$-based PVK top cell and an n-Si homojunction Si lower cell, resulting in an efficiency of 13.7%. Werner et al introduced homojunction Si capable of high-temperature heat treatment of TiO_2, which was used in the high-efficiency NIP PVK solar cell process.[58] In addition, by introducing a zinc tin oxide layer as a recombination layer, it was shown that the device was driven even after a 500°C heat treatment process. A 2T PVK/Si tandem solar cell was fabricated with this top cell and a bottom cell, and an efficiency of 16% was reported. Wu et al mentioned the merits of Si homojunction solar cells made by high-temperature processes, which are the mainstream in the existing solar cell market, and developed an n-Si-based homojunction PERL cells that maximize the long-wavelength absorption by controlling the refractive index of SiN_x.[59] A 2T PVK/Si tandem solar cell was fabricated by applying a PVK top cell based on NIP structure $Cs_{0.07}Rb_{0.03}FA_{0.765}MA_{0.135}PbI_{2.55}Br_{0.45}$ to the PERL bottom cell, and an efficiency of 22.5% was reported. Zheng et al demonstrated that SnO_2, which is used as an ETL in an NIP PVK top cell capable of low-temperature processing, can be introduced into a cell of n-Si homojunction PERL structure without a recombination layer.[60] Zheng et al applied SnO_2 as an ETL in an NIP $CH_3NH_3PbI_3$-based PVK top cell capable of low-temperature processing. This top cell was introduced on a cell with an n-Si homojunction PERL structure without an ITO layer, and the current matching point was determined by adjusting the thickness of $CH_3NH_3PbI_3$. In addition, the V_{oc} was also increased by heavy doping of the emitter of the Si bottom cell. The efficiencies of 2T PVK/Si tandem solar cells using these technologies were reported to be 20.5% at 4 cm^2 and 17.1% at 16 cm^2. Zheng

et al introduced $(FAPbI_3)_{0.83}(MAPbBr_3)_{0.17}$ and applied it to an n-Si-based homojunction Si solar cell with back side-texturing and reported efficiency of 21.8% at 16 cm^2 by introducing a new metal grid design.[61] Shen et al introduced TiO_2 ETL using the ALD process in $Cs_{0.05}Rb_{0.05}FA_{0.765}MA_{0.135}PbI_{2.55}Br_{0.45}$ based PVK solar cell with an NIP structure.[62] An efficiency of 24.1% was reported by developing a 2T PVK/Si tandem solar cell that minimized optical loss by introducing a TiO_2 layer using ALD in an n-Si-based homojunction Si lower cell. Zhu et al optimized high-quality PVK films by adjusting the ratio of *N,N*-dimetylformamide to dimethyl sulfoxide. A 2T PVK/Si tandem solar cell was fabricated with an NIP FAMACs PVK top cell with a high-quality PVK film and an n-Si heterojunction bottom cell.[63] As a result, the efficiency of the tandem solar cell was 22.80%. Zheng et al developed an ARC film that reduced optical loss and improved UV stability by applying a down-shifting material.[53] The 2T PVK/Si tandem solar cell was fabricated with an NIP structured PVK top cell and an n-Si homojunction bottom cell and reported an efficiency of 23.1%.

Representative 2T PVK/Si tandem solar cells based on an PIN structured PVK top cell and p-type homojunction Si bottom cell can be described as follows. Kanda et al deposited a transparent electrode on the opposite ends of the $CH_3NH_3PbI_3$-based PVK top cell and the p-Si homojunction Si bottom cell, and made a 2T PVK/Si tandem solar cell by mechanically contacting it to face each other and reported efficiency of 13.7%.[64] Hoye et al pointed out the possibility of commercialization of n-type Si solar cells used in tandem solar cells based on Si solar cells accounts for only 5% of the global solar cell market.[65] Using an PIN structured $CH_3NH_3PbI_3$-based PVK top cell, a 2T PVK/Si tandem solar cell was fabricated using a p-type Si-based bottom cell, and an efficiency of 16.2% was reported. Kanda et al reported efficiency of 15.5% by making a 2T PVK/Si tandem solar cell by mechanically contacting a $CH_3NH_3PbI_3$-based PVK top cell with a p-Si-based homojunction Si bottom cell that has increased efficiency through process optimization.[66] Based on the p-Si-based Al-BSF homojunction bottom cell, a mainstream of the solar cell market, a $(FAPbI_3)_{0.8}(MAPbBr_3)_{0.2}$ based PVK solar cell with an PIN structure, which has an HTL with an optimal band alignment, was tuned. As a result, the efficiency of the 2T PVK/Si tandem solar cell was 21.19%. Kanda et al introduced the texture of the bottom Si solar cell by adjusting the thickness of the PVK thin film of an NIP structured $CH_3NH_3PbI_3$-based PVK solar cell and reported efficiency of 15.9% by mechanically contacting it.[32] Choi et al developed a transparent conductive adhesive to mechanically bond the existing high-efficiency NIP structured PVK top cell and a p-Si-based Al-BSF homojunction bottom cell, which occupies the mainstream of the Si solar cell market.[67] In addition, a 2T PVK/Si tandem solar cell was fabricated based on an optical design that optimized the current density of a tandem solar cell in consideration of the refractive index of each layer, and an efficiency of 19.40% was reported.

Representative 2T PVK/Si tandem solar cells based on an NIP structured PVK top cell and an n-type heterojunction Si bottom cell are as follows. Werner et al fabricated an NIP structured $CH_3NH_3PbI_3$-based PVK top cell that minimized the light absorption by controlling the IZO thickness used as the recombination layer and the spiro-OMeTAD thickness of the HTL.[68] The 2T PVK/Si tandem solar cell made of this top cell on an n-Si heterojunction Si bottom cell reported efficiencies of 21.2% (0.17 cm^2) and 19.2% (1.22 cm^2). Albercht et al introduced SnO_2 ETL for low-temperature processing because the TiO_2 ETL layer used in an NIP structured PVK solar cell requires high-temperature heat treatment.[69] In this case, the passivation quality of the high-efficiency n-Si heterojunction Si bottom cell is degraded. This NIP structured $CH_3NH_3PbI_3$-based PVK top cell was applied to an n-Si heterojunction Si bottom cell, and an efficiency of 18% was reported. Werner et al introduced an n-Si heterojunction bottom cell with a rear texture introduced to increase long-wavelength absorption and applied this to an NIP structured $CH_3NH_3PbI_3$-based PVK top cell to fabricate a 2T PVK/Si tandem solar cell and reported an efficiency of 20.5%.[43] Bush et al introduced an PIN structured PVK solar cell with a wide bandgap using cesium formamidinium lead halide PVK and introduced a SnO_2 based buffer layer through ALD with minimized parasitic absorption, and showed excellent long-term stability.[70] A 2T PVK/Si tandem solar cell in which the top cell was introduced on an infrared-tuned n-Si heterojunction bottom cell was fabricated and reported efficiency of 23.6%. Fan et al made all of the NIP structure-based PVK by solution process.[71] $MA_{0.52}FA_{0.48}PbI_{2.937}Br_{0.063}$, $MA_{0.38}FA_{0.41}Cs_{0.21}PbI_{2.64}Br_{0.36}$, $MA_{0.37}FA_{0.48}Cs_{0.15}PbI_{2.01}Br_{0.99}$ PVK films, with bandgaps of 1.55, 1.61, and 1.69 eV respectively, were applied to an n-Si-based heterojunction Si bottom cell, and an efficiency of 20.57% was reported. Zhu et al introduced a transparent conducting oxide (TCO) layer that minimized the thickness of the MoO_x buffer layer and minimized the sputtering power condition to obtain high transmittance and applied it to a PVK top cell with an NIP structure.[72] This top cell was applied to an n-Si based heterojunction Si bottom cell to fabricate a 2 T PVK/Si tandem solar cell. An efficiency of 18.81% was reported without the ARC film. Qiu et al introduced a low-temperature process, with SnO_2 ETL and $FA_{0.5}MA_{0.38}Cs_{0.12}PbI_{2.04}Br_{0.96}$ having a bandgap of 1.69 eV, to fabricate an NIP structured PVK solar cell.[73] The solar cell was tandemized by applying the

layers to an n-Si-based heterojunction bottom cell, and an efficiency of 22.22% was reported. Sahli et al pointed out that recent 2T PVK/Si tandem solar cells use a TCO-based recombination layer that induces optical loss and reduces shunt resistance.[74] To solve this problem, a nanocrystalline Si oxide interlayer was introduced and the current density of the lower cell increased by 1 mA/cm^2. The 2T PVK/Si tandem solar cells which have an NIP structured PVK top cell with cesium-based PVK and an n-Si heterojunction bottom solar cells with nanocrystalline Si oxide interlayer, reported efficiencies of 22.0% at 0.25 cm^2 and 21.2% at 1.43 cm^2. Stannowski et al maximized the light absorption of the n-Si heterojunction bottom cell by inserting a nanocrystal Si oxide interlayer with a controlled refractive index between the ITO and Si layers.[75] A 2T PVK/Si tandem solar cell was fabricated by applying an NIP-structured top cell with $FA_{0.8}Cs_{0.5}MA_{0.5}Pb(I_xBr_{1-x})_3$ to the bottom cell, and an efficiency of 23.5% was reported. Bush et al proved that the pyramidal textured polydimethylsiloxane (PDMS) film exhibits a much better anti-reflection film effect than MgF_2, which was mainly used as an anti-reflection film layer in tandem solar cells.[76] The 2T PVK/Si tandem solar cells, which have $FA_{0.75}Cs_{0.25}Pb(I_{0.8}Br_{0.2})_3$ based PVK top cell with an PIN structure and an n-Si heterojunction bottom cell reported an efficiency of 25%. For the first time, Sahli et al reported efficiency of 25.2% by tandemizing an PIN structure PVK top cell through hybrid-type vacuum deposition on an n-Si-based double-sided textured heterojunction bottom solar cell.[77] Jošt et al reported an efficiency of 25.5% by applying a textured light management foil to a 2T PVK/Si tandem solar cell, which has a $Cs_{0.05}(MA_{0.17}FA_{0.83})Pb_{1.1}(I_{0.83}Br_{0.17})_3$ based PVK top cell with an PIN structure and an n-Si heterojunction bottom cell.[78] Hou et al fabricated an NIP structured PVK top cell using Cs to reduce the roughness of the FAMA-based PVK surface.[79] In addition, the V_{oc} of the n-Si heterojunction Si bottom cell was increased by optimizing the minority carrier lifetime by controlling the silane dilution ratio vs hydrogen. These cells were tandemized, and an efficiency of 20.43% was reported. Kim et al designed an optimized monolithic 2T PVK/Si tandem solar cell by considering each functional layer based on optical simulation.[54] Hou et al optimized the pyramid size of the pyramidally textured PDMS ARC film.[80] An efficiency of 21.93% was reported by applying an optimized ARC film by making a 2T PVK/Si tandem solar cell with an NIP structured PVK top cell and an n-Si heterojunction bottom cell. Kamino et al developed a low-temperature silver grid screen printing technology to replace the high-temperature screen printing technology used in the industry.[81] This technique was applied to a 2T PVK/Si tandem solar cell in which the n-Si heterojunction bottom cell and the $Cs_{0.17}FA_{0.83}PbI_{0.83}Br_{0.17}$ based PVK top cell with an PIN structure were tandemized, and 22.6% efficiency was reported at 57.4 cm^2. Park et al reported efficiency of 23.5% by optimizing the current matching of tandem solar cells using a 3T EQE analysis method and applying a $CH_3NH_3PbI_3$ based PVK top cell with an PIN structure to an n-Si heterojunction bottom cell.[82] Köhnen et al found that fill factor changes due to current mismatch in the 2T PVK/Si tandem solar cells.[22] In consideration of this, the $Cs_{0.05}(MA_{0.83}FA_{0.17})Pb(I_{0.83}Br_{0.17})_3$ based PVK top cell with an PIN structure and an n-Si heterojunction bottom cell were tandemized, and an efficiency of 25.0% was reported by minimizing the current mismatch. Nogay et al and Mazzarella et al reported an efficiency of 25.2% by adjusting the refractive index of nanocrystal Si-oxide to increase the absorption of long wavelengths of the n-Si heterojunction bottom cell, and tandemizing the PIN PVK top cell.[56,83] Chen et al reduced the V_{oc} deficit to 0.49 to 0.51 V through grain engineering that introduced MACl and MAH_2PO_2 into the PVK thin film.[84] This technology was applied to $Cs_{0.15}(FA_{0.83}MA_{0.17})_{0.85}Pb(I_{0.7}Br_{0.3})_3$ based PVK top cell with an PIN structure, and was tandemized with an n-Si heterojunction bottom cell, resulting in an efficiency of 25.4%. Hou et al, for the first time, demonstrated a tandem solar cell with a solution-process-based PVK top cell on the surface of a pyramid-textured Si bottom cell by adjusting the size of the texture pyramid on the surface of an existing industrial Si solar cell.[85] In addition, 1-butanethiol was introduced to overcome the limit of charge collection of the micro-thick PVK film formed on the pyramid texture surface, which increased the diffusion length, and prevented phase segregation. An efficiency of 25.7% was reported by tandemizing the $Cs_{0.05}MA_{0.15}FA_{0.8}PbI_{2.25}Br_{0.75}$ PVK top cell with an PIN structure, which has these technologies and an n-Si heterojunction bottom cell. Xu et al introduced triple-halide alloys using chlorine, bromine, and iodine to reduce the V_{oc} deficit caused by photo-induced phase segregation of wide band-gap PVK solar cells.[86] An efficiency of 27% was reported by tandemizing an PIN structured PVK top cell that applied this technology and an n-Si heterojunction bottom cell. Chen et al reduced the pyramid texture size and introduced a nitrogen-assisted blading process to successfully coat PVK with a thickness of 0.5 to 1 μm.[87] This technique was applied to an PIN structured PVK top cell and tandemized with an n-Si heterojunction bottom cell to report an efficiency of 26.2%. Kim et al fabricated a PVK top cell with 20.7% efficiency in 1.7 eV bandgap through anion engineering of phenethylammonium-based two-dimensional additives.[88] This was applied to an PIN structured PVK top cell and applied to the n-Si heterojunction bottom cell, and an efficiency of 26.7% was reported.

The 2T tandem solar cells based on an PIN structured PVK top cell and p-type heterojunction Si bottom cell are

described as follows. A double-sided textured p-Si heterojunction bottom cell was fabricated and tandemized with a PVK top cell with an PIN structure using a hybrid vacuum deposition process to report an efficiency of 25.1%.[83]

Recently, research on 2T PVK/Si tandem solar cells has developed rapidly, and many results have been reported in a short period of time. When the general tandem solar cell is divided into large and small areas based on 1 cm^2 (Figure 4A,B and Table S2), the largest area of reported PVK/Si tandem solar cell is 57.4 cm^2.[81] This showcases the importance of a large area technology for PVK top cells because it is considerably smaller than the area of a commercial silicon solar cell. The next chapter will introduce the fabrication process and electrode design of PVKs for large areas considering optical and electrical losses.

3 | SOLUTION AND EVAPORATION PROCESS FOR LARGE-SCALE PVK LAYER DEPOSITION

Among the solution processes such as spin coating, spray coating, slot-die coating, and the spin coating has been widely used for the deposition of PVK layers because of the easy control of the chemical composition and thickness to optimize PVK solar cells. In particular, the efficiency of PVK solar cells fabricated through spin coating began to increase rapidly after the advent of the anti-solvent dropping method, resulting in high-quality, dense, and pinhole-free PVK films.[89] However, in large-scale film coatings, spin coating is expensive because the material utilization rate is too low, and the spin coater is expensive to spin heavy substrates at high rotation speeds. In addition, nonuniform and insufficient anti-solvent coverage in PVK samples has made it difficult on a large scale to obtain high-quality, high-density, and pinhole-free PVK films with the anti-solvent dropping method. Unlike a spin coating, other solution processes such as spray coating, slot-die coating, and blade coating are suitable for large-scale PVK film deposition because they are easy to scale-up with continuous coating and have high material utilization (Figure 5).[90-92] However, many processing factors such as precursor, solvent, coating speed, and heating temperature must be optimized to achieve the same PVK film quality by spin coating. Zuo et al introduced a blow-assisted drop-casting method for $MAPbI_3$ films in air and achieved a champion PEC of 15.57% through a slot-die coating method with NH_4Cl additive to optimize the morphology of PVK films.[92] Cotella et al achieved a PCE of 9.2% by controlling the crystallization of PVK films using a slot die coating method with a preheated substrate and cold air knife.[93] Ulicna et al investigated PVK film morphology through a spray-coating process and anti-solvent dipping methods, resulting in a PCE of 17.29%.[94] Park et al developed a reproducible megasonic spray-coating method for $MAPbI_3$ film formation. With megasonic spray-coating, PVK films were prepared at low temperature with an anti-solvent-free process, resulting in a PCE of 14.2% in a 1 cm^2 active area.[95] Recently, a high-efficiency PVK solar module using a large-scale solution process rather than spin coating has been reported through process factor optimization and the development of a new method. Currently, 11.1% PCE of 168.75 cm^2 PVK module and 16.9% PCE of 63.7 cm^2 size by slot-die coating and blade coating have been reported, respectively.[96,97] The previous results are quite promising, but the PVK compositions are both simple $MAPbI_3$, and control of PVK composition in a

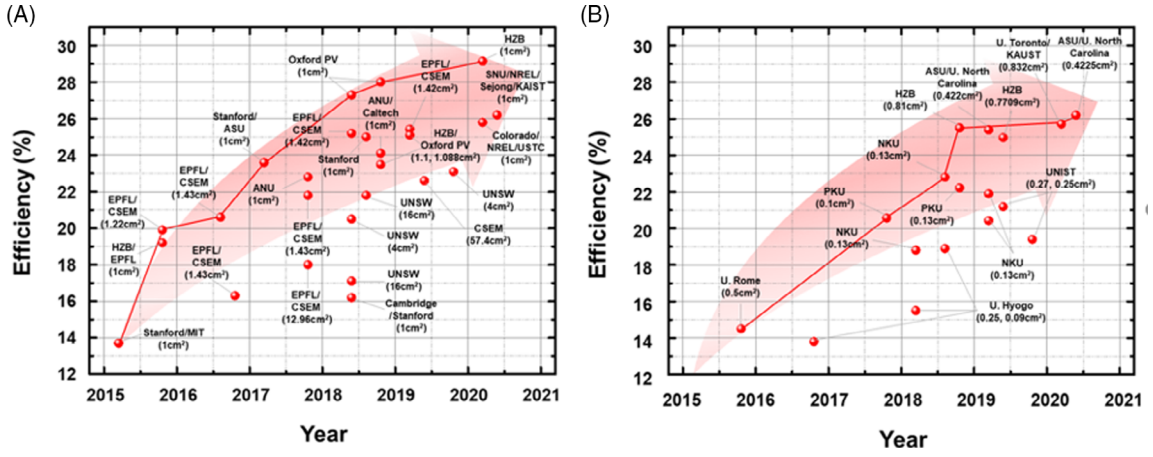

FIGURE 4 The efficiency chart of reported 2-terminal PVK/Si tandem solar cell; (A) active area of tandem device ≥1 cm^2 (B) active area of tandem device <1cm^2

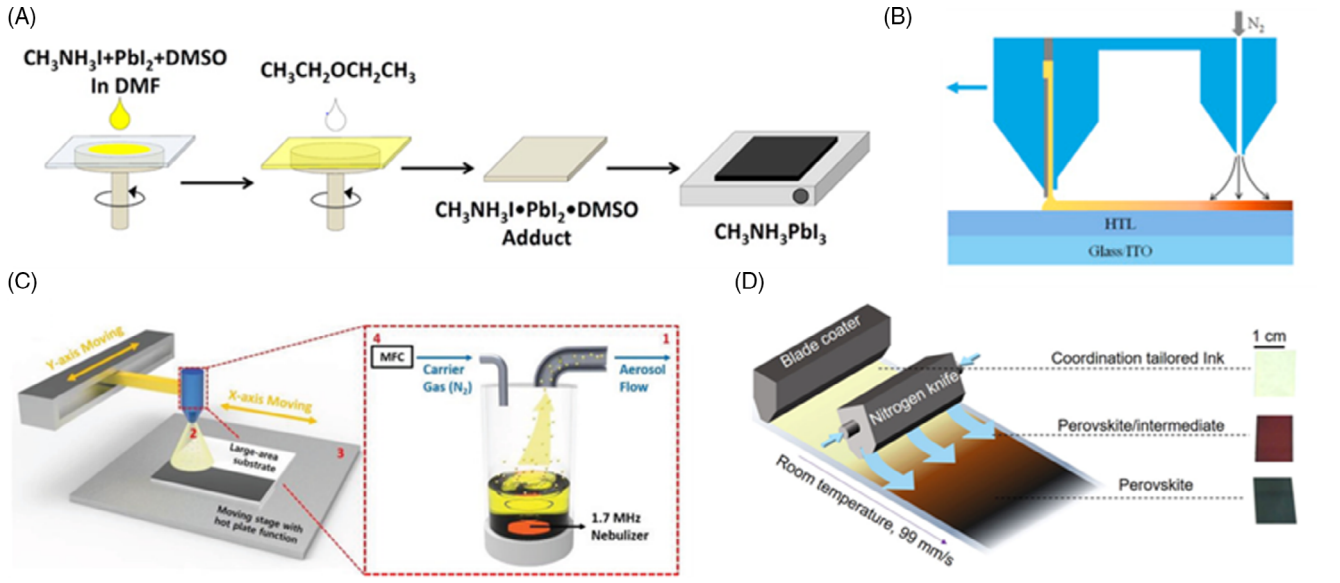

FIGURE 5 Schematic illustration for (A) spin coating process with anti-solvent washing. Reproduced with permission: Copyright 2015, American Chemical Society.[89] (B) Slot-die coating process. Reproduced with permission: Copyright 2018, Elsevier.[92] (C) spray coating process. Reproduced with permission: Copyright 2019, John Wiley and Sons.[95] (D) Blade coating process. Reproduced with permission: Copyright 2019, American Association for the Advancement of Science[97]

large-scale solution process is required to optimize the bandgap of PVK and increase the efficiency of PVK/Si tandem solar cell.

While the solution process has been mainly used for PVK layer coating until now, the evaporation process for PVK layer coating is also continuously being studied because the evaporation process provides highly uniform and pinhole-free films even in a large area (Figure 6).[98-100] Basically, organometal halide PVKs are chemical compounds that are usually synthesized by the reaction of metal halides with organic ammonium halides. As organometal halide PVK easily decomposes at high temperature and vacuum conditions, instead of evaporating organometal halide PVK itself, the two components of organometal halide PVK evaporate to form a PVK layer. There are two common ways to evaporate two components of PVK: one is a one-step co-evaporation method, and the other is a two-step sequential evaporation method. However, the vapor pressure of organic ammonium halides under vacuum conditions is so high that unstable vacuum deposition and the absence of solvent that helps the reaction between the two components have hindered the achievement of a high-quality PVK layer during the evaporation process. At first time, the hybrid process that using evaporation process for inorganic components and solution process for organic components on inorganic components were introduced for large-scale PVK/Si tandem solar cells.[68,74,77] This hybrid process has advantages of both evaporation process and solution process, which shows uniform and pinhole-free PVK films with easy control of chemical composition. However, in-line process for mass production is not possible in hybrid process and optimization of both evaporation process and solution process is too complex. In order to overcome the limitations of hybrid process, all evaporation process for large-scale PVK layer deposition has been researched continuously. Zheng et al studied the effect of solvent annealing on grain growth in 2D PVKs prepared by single-source thermal evaporation, and through solvent annealing, the crystallinity of 2D PVKs was improved, and a PCE of 4.67% was achieved.[101] Lei et al first formed a PbI_2 layer by normal evaporation and then fabricated MAI by flash evaporation to obtain a homogeneous large-scale PVK film. All evaporated PVK devices achieved a champion PCE of 15.06% at 16 cm^2 active area.[102] By optimizing the evaporation process parameters such as deposition rate, substrate temperature, chamber pressure, etc., PCEs of more than 20% have recently been reported with co-evaporated PVK layers.[103] Moreover, 18.13% PCE of a 21 cm^2 PVK module by co-evaporation method was reported.[104] However, to optimize the bandgap of PVK and increase the efficiency of PVK/Si tandem solar cells, uniformity and control of PVK composition in large-scale evaporation processes are also required. Notably, newly developed evaporation processes, such as flash evaporation and closed-space vapor transport, can be an innovative breakthrough to overcome the decomposition problem of PVK materials.[105,106] Applying a newly developed evaporation process and optimizing the parameters in the evaporation process will

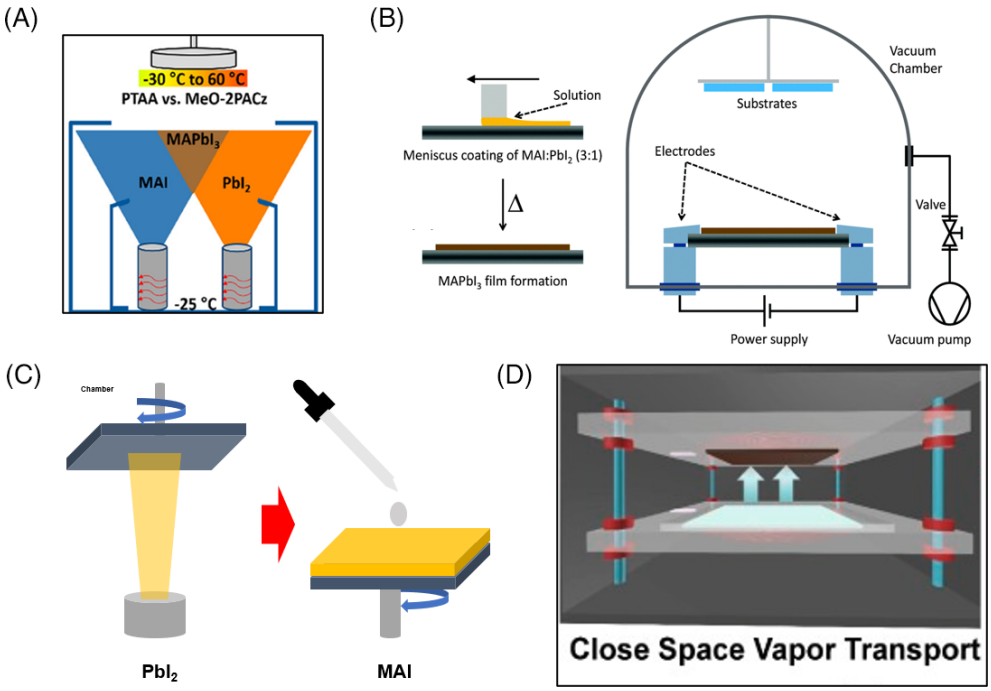

FIGURE 6 Schematic illustration of (A) PVK co-evaporation method with controlling substrate temperature. Reproduced with permission: Copyright 2020, American Chemical Society.[103] (B) Flash evaporating method. Reproduces with permission: Copyright 2015, Royal Society of Chemistry.[105] (C) Two-step sequential process. (D) Close space evaporation process. Reproduces with permission: Copyright 2016, John Wiley and Sons[106]

enable uniform single-source deposition of PVK composition optimized for PVK/Si tandem solar cells.

4 | CHALLENGES AND PROGRESS IN LARGE-SCALE PVK/Si TANDEM SOLAR CELLS

Undoubtedly, a high-quality and pinhole-free PVK layer by the scalable deposition process mentioned above is necessary for efficient large-scale PVK/Si tandem solar cells. However, it is not the only obstacle to scale up PVK/Si tandem solar cells. The first step to consider in large-scale PVK/Si tandem solar cells is the recombination layer. In the 2T monolithic PVK/Si tandem solar cell, the vertical resistance of the recombination layer should be low enough to connect the bottom and top cells without resistance loss, and the TCOs were utilized as recombination layers owing to their intrinsic high transparency and low resistance. However, defects in the PVK layer or charge transport layers (CTL) are inevitable in large-scale PVK/Si tandem solar cell fabrication, and the shunting effect due to pinholes and defects is important for the failure of large-scale PVK/Si tandem solar cells. To prevent the failure of large-scale PVK/Si tandem solar cells, it is necessary to increase the lateral resistance of the recombination layer to localize the shunting effect and minimize leakage current. An important step for large-scale PVK/Si tandem solar cells is the development of a high lateral resistance recombination layer (Figure 7). In PVK/Si tandem solar cells 19.1% PCE of 12.96 cm^2 was achieved using p+/n+ hydrogenated nanocrystalline silicon recombination junction deposited by plasma-enhanced chemical vapor deposition instead of TCO.[74] In addition, 17.6% PCE of 16 cm^2 PVK/Si tandem solar cell was achieved through the optimized conductivity of recombination layer formed by the combination of a doping-level control emitter and a solution-processed charge-selective metal oxide nanoparticle layer.[60]

However, the lateral resistance of the transparent electrode should be low to collect the generated charge carrier efficiently to the external circuit without loss, while the lateral resistance of the recombination layer should be low in large-scale PVK/Si tandem solar cells. After the introduction of a metal-oxide-based sputtering damage buffer layer, TCOs with high transparency and conductivity were sputtered as the top transparent electrode of PVK/Si tandem solar cells, but TCO itself has limitations as the top transparent electrode that conflicts with electrical conductivity and transparency.

To overcome the limitations of TCO itself, the sheet resistance of the transparent electrode was effectively reduced by using a metal grid on top of TCO. To obtain a low resistance of a transparent electrode with a metal grid, a metal with low resistivity, a short distance between the metal fingers, and a large cross-sectional area of the metal finger are desirable. However, the light-shading loss caused by the top surface of the metal grid prevents light from entering the solar cell and limits the increase in efficiency by introducing a metal grid. Therefore, for efficient large-scale PVK/Si tandem solar cells, optimal metal grid design, and metal finger height-to-

width aspect ratio (geometry) are required (Figure 8). It was reported that the PCE of a PVK/Si tandem solar cell with 16 cm^2 size increased from 17.6 to 21.8% after metal grid design optimization.[60,61] It was also reported that shading loss decreased to less than 0.8% after increasing the metal finger aspect ratio using a graded-opening shadow mask.[86]

5 | OBSTACLES FOR COMMERCIALIZATION AND OUTLOOK

Recently, the record efficiencies of 2T PVK/Si tandem solar cells are expected to exceed 30%, and the area of large-scale PVK layer deposition process has become large enough to cover the size of commercial silicon solar cell wafers. Although the efficiency of 2T PVK/Si tandem solar cells is higher than 29%, which is the theoretical limit of Si single-junction solar cells, and the rapid development of large-scale deposition processes for PVK layers are promising, the cost of PVK/Si tandem solar cells should be considered for commercialization. According to the recently reported cost analysis for PVK solar cells and PVK/Si tandem solar cells, the process equipment and maintenance costs of the evaporation process may be low with high throughput in mass production. PVK solar cells have generally reported high material cost issues rather than processing costs in cost analysis. In particular, the cost barrier of PVK solar cells is identified by expensive organic charge transport materials such as spiro-OMeTAD, PTAA, and $PC_{60}BM$.[107-109] The cost of high-performance organic charge transport materials is usually expensive owing to the complex synthesis steps and additional cost for ultra-high purity. As an alternative, the cost of inorganic charge transport materials such as NiO, CuSCN, SnO_2, and Nb_2O_5 is much cheaper than organic materials, and several large-scale compatible processed inorganic CTLs have been reported in PVK solar cells (Figure 9A).[110-113]

From the perspective of eco-friendly renewable energy, it is necessary to solve the toxicity and longevity of PVK/Si tandem solar cells, which are the drawbacks of PVK, to gain an advantage over other energy sources. Most PVK solar cells are based on toxic lead (Pb) due to their excellent optoelectronic properties. Although the total amount of Pb in PVK/Si tandem solar cells is very low, it has been reported that the Pb of halide PVK is 10 times more dangerous than the Pb that already exists on the earth.[114] To lower its toxicity, Pb-free and less-Pb PVK based solar cells have been researched using safe tin (Sn)-based PVK.[115-117] However, Sn-based PVK solar cells have lower efficiencies and faster degradation than Pb-based PVK solar cells due to phase instability and easy oxidation from Sn^{2+} to Sn^{4+}. In addition, new approaches have been suggested to prevent Pb leakage in PVK solar modules by trapping Pb with cation-exchange resins containing abundant and inexpensive Ca^{2+} and Mg^{2+}.[118]

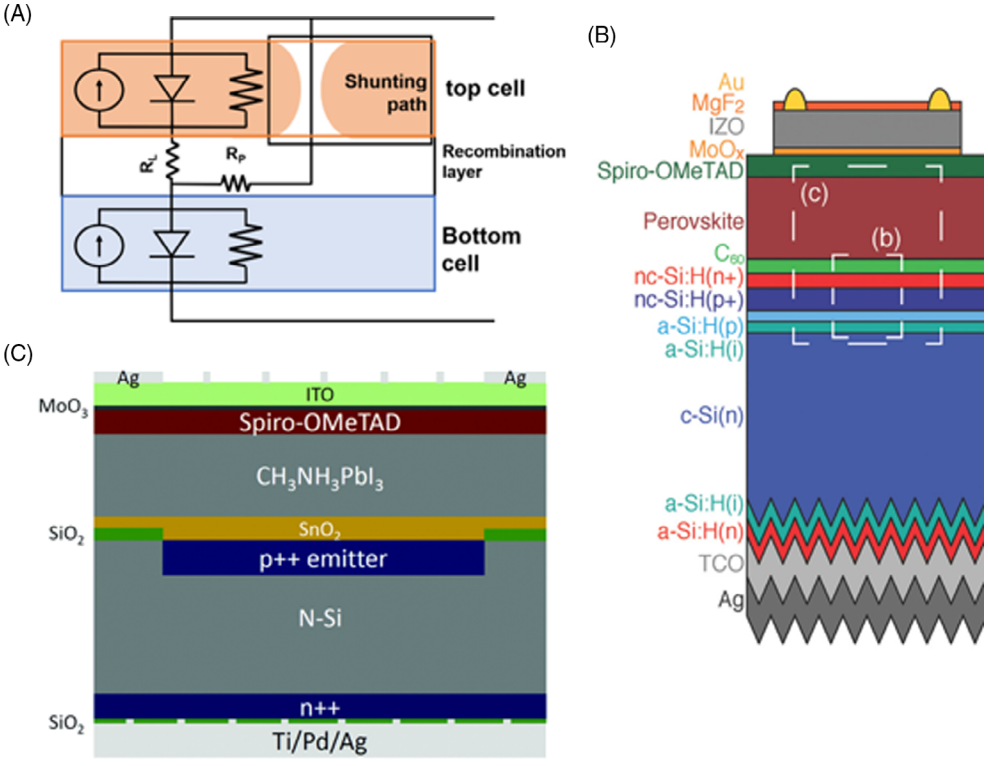

FIGURE 7 (A) Schematic of perovskite/Si tandem solar cell with a recombination layer shunting path. (B) Device sturcture of PVK/Si tandem solar cells with p+/n + hydrogenated nanocrystalline silicon recombination junction. Reproduces with permission: Copyright 2018, John Wiley and Sons.[74] (C) Device sturcture of PVK/Si tandem solar cells with doping-level control emitter and a solution-processed chargeselective metal oxide nanoparticle. Reproduces with permission: Copyright 2018, Royal Society of Chemistry[60]

Solar cells are exposed to degradation sources such as moisture, oxygen, heat, and ultraviolet light in actual use, and to ensure the long lifetime of PVK/Si solar cells, the stability of PVK solar cells against the degradation sources should be further increased.[119-121] To solve the easy decomposition of methylammonium lead triiodide

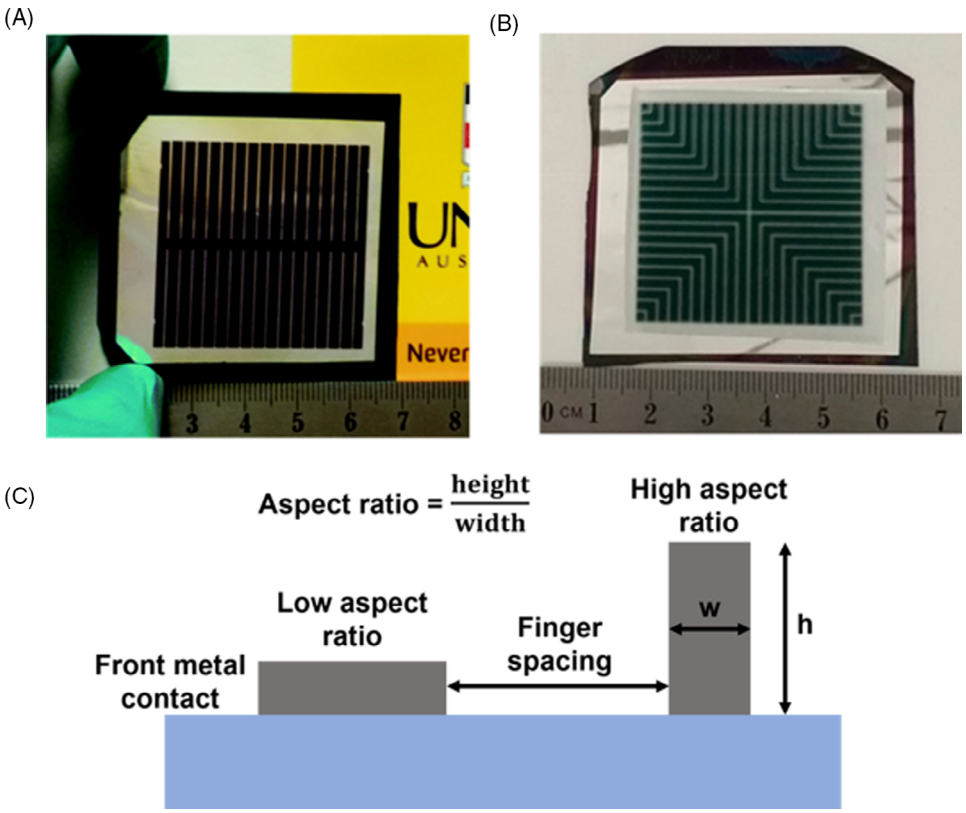

FIGURE 8 (A) Photograph of large-scale PVK/Si tandem solar cell with metal grid. Reproduces with permission: Copyright 2018, Royal Society of Chemistry.[60] (B) Photograph of large-scale PVK/Si tandem solar cell with optimal metal grid design. Reproduces with permission: Copyright 2018, American Chemical Society.[61] (C) Scheme illustration of a metal finger height-to-width aspect ratio and spacing

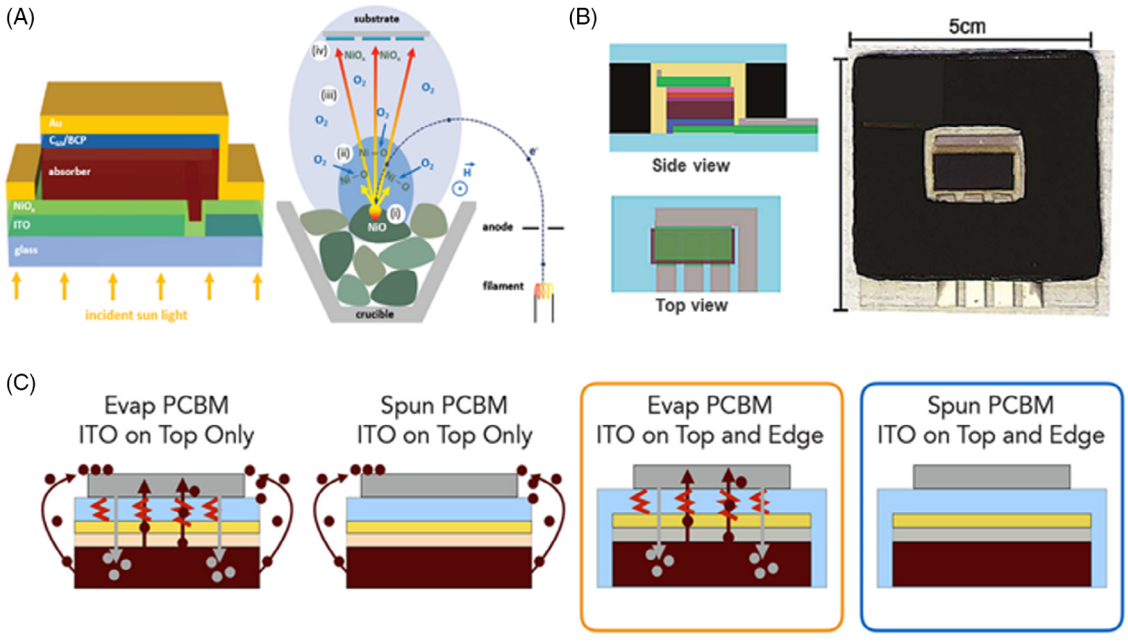

FIGURE 9 (A) PVK solar cell with NiO as inorganic CTL, Reproduced with permission: Copyright 2019, John Wiley and Sons.[110] (B) Schematic side and top views of encapsulation package and photograph of PVK solar cell after encapsulation. Reproduces with permission: Copyright 2018, Royal Society of Chemistry.[125] (C) Schematics of metal and halide diffusion in PVK solar cells with different inorganic diffusion barrier structures. Reproduces with permission: Copyright 2018, American Chemical Society[126]

PVK by moisture and heat, optimized PVK compositions were developed by mixing cations and halogen anions to achieve high stability against moisture and heat. Unlike thermally decomposed metylammonium lead triiodide PVK, formamidinium lead triiodide PVK, and cesium lead triiodide PVK showed high resistance to thermal decomposition. By mixing the cations, the thermal stability of PVK improved as well as crystal phase stability. For halide anions, Bromide-based PVK showed higher stability against moisture and heat than the iodide-based PVK, and the PVK composition was further optimized by mixing both halogens for better stability. Further optimization of the PVK composition by incorporating equivalent small metal ions and forming 2D/3D hetero-structured PVK to increase stability have been reported.[122-124] It is well known that organic charge transport materials are easily decomposed by moisture and oxygen and require a high level of encapsulation. Inorganic charge transport materials are generally advantageous for stability owing to their original robust properties. Moreover, it was reported that a densely formed inorganic layer could act as a diffusion barrier to prevent the escape of volatiles, and the thermal stability of PVK solar cells with an inorganic layer was significantly improved. It was reported that a semi-transparent PVK solar cell, with a densely formed CTL and transparent electrode, passed the thermal cycling test, damp heat test, and UV stress test (Figure 9B,C).[125-127]

Although the above obstacles in the commercialization of PVK/Si tandem solar cells have been discussed in detail in the literature and many potential solutions have been suggested, the high processing temperature of top metal grid metallization of conventional Si solar cells has been overlooked. Large-scale solar cells require a low series resistance of the top electrode, which requires metallization of the top metal grid. However, screen printing that requires a high temperature of 800°C in a Si solar cell is not possible in PVK solar cells, where conventional silver paste metallization is susceptible to heat. In heterojunction Si solar cells, low-temperature plating metallization was developed to prevent degradation of a-Si:H based passivated contacts, but for PVK solar cells vulnerable to moisture, the plating process immersed in a bath with metal salt is also impossible. Although a metal grid was formed on a PVK/Si tandem solar cell by evaporation, its material utilization rate is too low, and high usage of Ag significantly increases the total cost. Recently, a cold metallization process suitable for PVK solar cells was developed from low-temperature cell connection technology, the so-called SmartWire Connection Technology developed by Meyer-Burger.[128] It is a simple lamination process between metal wire embedded polymer foil and the top surface of the solar cell. Low melting-point alloy layer coated copper wire can be used to reduce the wire interconnection temperature to 160°C or less. In this SmartWire Connection Technology, both material usage and optical shading loss can be reduced in conventional wide busbars by optimizing the grid design and wire geometry, and further improvement of PVK/Si tandem solar cell for commercialization should be considered in this new approach.

6 | CONCLUSION

In this review, we summarize large-scale monolithic PVK/Si tandem solar cells with representative structures of Si-based PVK tandem solar cells, optical and electrical development of PVK/Si tandem solar cells, the process of large-scale PVK solar cells, and challenges of large-scale PVK/Si tandem solar cells. In the 4T tandem solar cell, optical loss of tandem solar cell exists due to the air gap between the PVK top cell and the Si bottom cell. However, as the 2T tandem solar cell is a simple integrated type, it has the advantage of less parasitic absorption but requires a technique such as current matching. Optical and electrical developments have been studied to achieve high-efficiency PVK/Si tandem solar cells. To overcome the reduction in efficiency due to optical loss, a textured surface is used to reduce the reflections between interlayers and optimize the transmittance and conductivity of the top electrode. Meanwhile, electrical properties are improved by many processes, such as the introduction of a sputtering buffer layer. For the commercialization of PVK/Si tandem solar cells, the optical and electrical properties must be improved, and the development of a large-scale PVK layer deposition process is critical. Recently, the spin coating process has been widely used in the solution process by easily controlling the chemical composition, forming a high-quality and high-density PVK film by anti-solvent dropping, and optimizing the thickness and bandgap of the PVK layer. However, spin coating is not suitable for large-scale processes. Therefore, other solution processes, such as spray coating, slot-die coating, and blade coating, were mainly used in large-scale PVK solar cells. A dense and pinhole-free PVK film can be easily formed during the evaporation process, but the control of chemical reactions between organic cations and metal halides is very difficult. Various processes have been developed during the evaporation process, including substrate temperature control, flash evaporation, two-step sequential process, and proximity evaporation to form high-quality PVK layers. However, in PVK/Si tandem solar cells, scale-up is not the only obstacle, but the recombination layer resistance control is also important. The vertical resistance should

be low to prevent electrical loss of the recombination layer, but the lateral resistance of the recombination layer should be high to eliminate the shunting path. To overcome the limitation of the TCO layer, the properties of metal grids such as low resistivity metal, short distance between the metal fingers, and large cross-sectional area of metal fingers are important. However, PVK/Si tandem solar cells have to overcome several obstacles to commercialization. The commercialization of PVK solar cells with the high material cost is being pointed out, and the toxicity and stability of PVK materials are critical issues for commercialization. Additionally, conventional unfeasible metallization temperatures for PVK/Si tandem solar cells are being overlooked, and these hurdles must be overcome to commercialize PVK/Si tandem solar cells.

ACKNOWLEDGMENTS

Chan Ul Kim, Eui Dae Jung, and Young Wook Noh contributed equally to this work. This work was supported by the Korea Institute of Energy Technology Evaluation and Planning (KETEP) and the Ministry of Trade, Industry & Energy (MOTIE) of Republic of Korea (No. 20163010012450). This work was supported by Korea Institute of Energy Technology Evaluation and Planning (KETEP) grant funded by the Korea government (MOTIE) (20193091010460, Development of Super Solar cells for overcoming the theoretical limit of silicon solar cell efficiency [>30%]). This work was supported by the Technology Development Program to Solve Climate Changes through the National Research Foundation of Korea (NRF) funded by the Ministry of Science and ICT (2019M1A2A2072416). This work was also supported by the 2020 Research Fund of KOREA East-West Power Co., LTD. (EWP) (2.190433.01).

ORCID

Myoung Hoon Song https://orcid.org/0000-0002-8106-7332

REFERENCES

1. Philipps S, Warmuth W. Photovoltaics report—Fraunhofer ISE; 2020.
2. Saga T. Advances in crystalline silicon solar cell technology for industrial mass production. *NPG Asia Mater*. 2010;2:96-102.
3. Qiu L, Ono LK, Qi Y. Advances and challenges to the commercialization of organic–inorganic halide perovskite solar cell technology. *Mater Today Energy*. 2018;7:169-189.
4. Tawada Y, Yamagishi H. Mass-production of large size a-Si modules and future plan. *Sol Energy Mater Sol Cells*. 2001;66:95-105.
5. Reichelstein S, Yorston M. The prospects for cost competitive solar PV power. *Energy Policy*. 2013;55:117-127.
6. Zhou Y, Fuentes-Hernandez C, Khan TM, et al. Recyclable organic solar cells on cellulose nanocrystal substrates. *Sci Rep*. 2013;3:1536.
7. Fischer M, Woodhouse M, Herritsch S, et al. International Technology Roadmap for Photovoltaic (ITRPV) Result 2019 including maturity report 2020; 2020.
8. Smith DD, Cousins P, Westerberg S, Jesus-Tabajonda RD, Aniero G, Shen YC. Toward the practical limits of silicon solar cells. *IEEE J Photovolt*. 2014;4:1465-1469.
9. Yamaguchi M, Takamoto T, Araki K, Ekins-Daukes N. Multi-junction III–V solar cells: current status and future potential. *Sol Energy*. 2005;79:78-85.
10. Takamoto T, Washio H, Juso H. Application of InGaP/GaAs/InGaAs triple junction solar cells to space use and concentrator photovoltaic. 2014 IEEE 40th Photovoltaic Specialist Conference (PVSC); 2014; 0001-0005. https://doi.org/10.1109/PVSC.2014.6924936
11. Fthenakis VM, Bowerman B. Environmental health and safety (EHS) issues in III-V solar cell manufacturing. Proceeding of 3rd World Conference on Photovoltaic Energy Conversion; 2003; Vol 1. 681-684.
12. Jain N, Hudait MK. III–V multijunction solar cell integration with silicon: present status, challenges and future outlook. *Energy Harvest Syst*. 2014;1:121-145.
13. Li K, Li Z, Feng K, Xu X, Wang L, Peng Q. Development of large band-gap conjugated copolymers for efficient regular single and tandem organic solar cells. *J Am Chem Soc*. 2013;135:13549-13557.
14. Kwon J, Im MJ, Kim CU, et al. Two-terminal DSSC/silicon tandem solar cells exceeding 18% efficiency. *Energ Environ Sci*. 2016;9:3657-3665.
15. Wang Z, Song Z, Yan Y, et al. Perovskite—a perfect top cell for tandem devices to break the S–Q limit. *Adv Sci*. 2019;6:1801704.
16. Bailie CD, Christoforo MG, Mailoa JP, et al. Semi-transparent perovskite solar cells for tandems with silicon and CIGS. *Energ Environ Sci*. 2015;8:956-963.
17. Meng L, Zhang Y, Wan X, et al. Organic and solution-processed tandem solar cells with 17.3% efficiency. *Science*. 2018;361:1094-1098.
18. Al-Ashouri A, Magomedov A, Roß M, et al. Conformal monolayer contacts with lossless interfaces for perovskite single junction and monolithic tandem solar cells. *Energ Environ Sci*. 2019;12:3356-3369.
19. Chen X, Jia Z, Chen Z, et al. Efficient and reproducible monolithic Perovskite/organic tandem solar cells with low-loss interconnecting layers. *Joule*. 2020;4:1594-1606.
20. Lin R, Xiao K, Qin Z, et al. Monolithic all-perovskite tandem solar cells with 24.8% efficiency exploiting comproportionation to suppress Sn(II) oxidation in precursor ink. *Nat Energy*. 2019;4:864-873.
21. Al-Ashouri A, Köhnen E, Li B, et al. Monolithic perovskite/silicon tandem solar cell with >29% efficiency by enhanced hole extraction. *Science*. 2020;370:1300-1309.
22. Köhnen E, Jošt M, Morales-Vilches AB, et al. Highly efficient monolithic perovskite silicon tandem solar cells: analyzing the influence of current mismatch on device performance. *Sustain Energy Fuels*. 2019;3:1995-2005.
23. Filipič M, Löper P, Niesen B, et al. CH3NH3PbI3 perovskite/silicon tandem solar cells: characterization based optical simulations. *Opt Express*. 2015;23:A263-A278.

24. Jiang Y, Almansouri I, Huang S, et al. Optical analysis of perovskite/silicon tandem solar cells. *J Mater Chem C*. 2016;4:5679-5689.
25. Qian J, Ernst M, Wu N, Blakers A. Impact of perovskite solar cell degradation on the lifetime energy yield and economic viability of perovskite/silicon tandem modules. *Sustain Energy Fuels*. 2019;3:1439-1447.
26. Cho Y, Soufiani AM, Yun JS, et al. Mixed 3D–2D passivation treatment for mixed-cation lead mixed-halide perovskite solar cells for higher efficiency and better stability. *Adv Energy Mater*. 2018;8:1703392.
27. Bush KA, Frohna K, Prasanna R, et al. Compositional engineering for efficient wide band gap perovskites with improved stability to photoinduced phase segregation. *ACS Energy Lett*. 2018;3:428-435.
28. Kothandaraman RK, Jiang Y, Feurer T, Tiwari AN, Fu F. Near-infrared-transparent perovskite solar cells and perovskite-based tandem photovoltaics. *Small Methods*. 2020;4:2000395.
29. Hu J, Cheng Q, Fan R, Zhou H. Recent development of organic–inorganic Perovskite-based tandem solar cells. *Sol RRL*. 2017;1:1700045.
30. Hörantner MT, Snaith HJ. Predicting and optimising the energy yield of perovskite-on-silicon tandem solar cells under real world conditions. *Energ Environ Sci*. 2017;10:1983-1993.
31. Aydin E, De Bastiani M, Yang X, et al. Zr-doped indium oxide (IZRO) transparent electrodes for Perovskite-based tandem solar cells. *Adv Funct Mater*. 2019;29:1901741.
32. Kanda H, Shibayama N, Uzum A, et al. Effect of silicon surface for perovskite/silicon tandem solar cells: flat or textured? *ACS Appl Mater Interfaces*. 2018;10:35016-35024.
33. Wang Z, Zhu X, Zuo S, et al. 27%-efficiency four-terminal perovskite/silicon tandem solar cells by sandwiched gold nanomesh. *Adv Funct Mater*. 2020;30:1908298.
34. Duong T, Lal N, Grant D, et al. Semitransparent perovskite solar cell with sputtered front and rear electrodes for a four-terminal tandem. *IEEE J Photovolt*. 2016;6:679-687.
35. Ren Z, Zhou J, Ng A, et al. Record high performance of perovskite/crystalline silicon four-terminal tandem solar cells. 2016 IEEE 43rd Photovoltaic Specialist Conference (PVSC); 2016; 0816-0820. https://doi.org/10.1109/PVSC.2016.7749719.
36. Ren Z, Zhou J, Zhang Y, et al. Strategies for high performance perovskite/crystalline silicon four-terminal tandem solar cells. *Sol Energy Mater Sol Cells*. 2018;179:36-44.
37. Dewi HA, Wang H, Li J, et al. Highly efficient semitransparent perovskite solar cells for four terminal perovskite-silicon tandems. *ACS Appl Mater Interfaces*. 2019;11:34178-34187.
38. Najafi M, Zardetto V, Zhang D, et al. Highly efficient and stable semi-transparent p-i-n planar perovskite solar cells by atmospheric pressure spatial atomic layer deposited ZnO. *Sol RRL*. 2018;2:1800147.
39. Ramírez Quiroz CO, Shen Y, Salvador M, et al. Balancing electrical and optical losses for efficient 4-terminal Si–perovskite solar cells with solution processed percolation electrodes. *J Mater Chem A*. 2018;6:3583-3592.
40. Duong T, Pham H, Kho TC, et al. High efficiency perovskite-silicon tandem solar cells: effect of surface coating versus bulk incorporation of 2D perovskite. *Adv Energy Mater*. 2020;10:1903553.
41. Löper P, Moon S-J, Martín de Nicolas S, et al. Organic–inorganic halide perovskite/crystalline silicon four-terminal tandem solar cells. *Phys Chem Chem Phys*. 2015;17:1619-1629.
42. Werner J, Dubuis G, Walter A, et al. Sputtered rear electrode with broadband transparency for perovskite solar cells. *Sol Energy Mater Sol Cells*. 2015;141:407-413.
43. Werner J, Barraud L, Walter A, et al. Efficient near-infrared-transparent perovskite solar cells enabling direct comparison of 4-terminal and monolithic perovskite/silicon tandem cells. *ACS Energy Lett*. 2016;1:474-480.
44. Yang M, Kim DH, Yu Y, et al. Effect of non-stoichiometric solution chemistry on improving the performance of wide-bandgap perovskite solar cells. *Mater Today Energy*. 2018;7:232-238.
45. Zhang D, Najafi M, Zardetto V, et al. High efficiency 4-terminal perovskite/c-Si tandem cells. *Sol Energy Mater Sol Cells*. 2018;188:1-5.
46. Jaysankar M, Filipič M, Zielinski B, et al. Perovskite–silicon tandem solar modules with optimised light harvesting. *Energ Environ Sci*. 2018;11:1489-1498.
47. Jaysankar M, Raul BAL, Bastos J, et al. Minimizing voltage loss in wide-bandgap perovskites for tandem solar cells. *ACS Energy Lett*. 2019;4:259-264.
48. Gharibzadeh S, Hossain IM, Fassl P, et al. 2D/3D heterostructure for semitransparent perovskite solar cells with engineered bandgap enables efficiencies exceeding 25% in four-terminal tandems with silicon and CIGS. *Adv Funct Mater*. 2020;30:1909919.
49. Rohatgi A, Zhu K, Tong J, et al. 26.7% efficient 4-terminal perovskite–silicon tandem solar cell composed of a high-performance semitransparent Perovskite cell and a doped poly-Si/SiOx passivating contact silicon cell. *IEEE J Photovolt*. 2020;10:417-422.
50. Dewi HA, Wang H, Li J, et al. Four-terminal perovskite on silicon tandem solar cells optimal measurement schemes. *Energ Technol*. 2020;8:1901267.
51. Leijtens T, Bush KA, Prasanna R, McGehee MD. Opportunities and challenges for tandem solar cells using metal halide perovskite semiconductors. *Nat Energy*. 2018;3:828-838.
52. Ou Q, Bao X, Zhang Y, et al. Band structure engineering in metal halide perovskite nanostructures for optoelectronic applications. *Nano Mater Sci*. 2019;1:268-287.
53. Zheng J, Mehrvarz H, Liao C, et al. Large-area 23%-efficient monolithic perovskite/homojunction-silicon tandem solar cell with enhanced UV stability using Down-shifting material. *ACS Energy Lett*. 2019;4:2623-2631.
54. Kim CU, Yu JC, Jung ED, et al. Optimization of device design for low cost and high efficiency planar monolithic perovskite/silicon tandem solar cells. *Nano Energy*. 2019;60:213-221.
55. Bett AJ, Schulze PSC, Winkler KM, et al. Two-terminal perovskite silicon tandem solar cells with a high-bandgap Perovskite absorber enabling voltages over 1.8 V. *Prog Photovolt*. 2020;28:99-110.
56. Mazzarella L, Lin Y-H, Kirner S, et al. Infrared light management using a nanocrystalline silicon oxide interlayer in monolithic perovskite/silicon heterojunction tandem solar cells with efficiency above 25%. *Adv Energy Mater*. 2019;9:1803241.

57. Mailoa JP, Bailie CD, Johlin EC, et al. A 2-terminal perovskite/silicon multijunction solar cell enabled by a silicon tunnel junction. *Appl Phys Lett*. 2015;106:121105.
58. Werner J, Walter A, Rucavado E, et al. Zinc tin oxide as high-temperature stable recombination layer for mesoscopic perovskite/silicon monolithic tandem solar cells. *Appl Phys Lett*. 2016;109:233902.
59. Wu Y, Yan D, Peng J, et al. Monolithic perovskite/silicon-homojunction tandem solar cell with over 22% efficiency. *Energ Environ Sci*. 2017;10:2472-2479.
60. Zheng J, Lau CFJ, Mehrvarz H, et al. Large area efficient interface layer free monolithic perovskite/homo-junction-silicon tandem solar cell with over 20% efficiency. *Energ Environ Sci*. 2018;11:2432-2443.
61. Zheng J, Mehrvarz H, Ma F-J, et al. 21.8% efficient monolithic perovskite/homo-junction-silicon tandem solar cell on 16 cm2. *ACS Energy Lett*. 2018;3:2299-2300.
62. Shen H, Omelchenko ST, Jacobs DA, et al. In situ recombination junction between p-Si and TiO2 enables high-efficiency monolithic perovskite/Si tandem cells. *Sci Adv*. 2018;4: eaau9711.
63. Zhu S, Hou F, Huang W, et al. Solvent engineering to balance light absorbance and transmittance in perovskite for tandem solar cells. *Sol RRL*. 2018;2:1800176.
64. Kanda H, Uzum A, Nishino H, et al. Interface optoelectronics engineering for mechanically stacked tandem solar cells based on perovskite and silicon. *ACS Appl Mater Interfaces*. 2016;8: 33553-33561.
65. Hoye RLZ, Bush KA, Oviedo F, et al. Developing a robust recombination contact to realize monolithic perovskite tandems with industrially common p-type silicon solar cells. *IEEE J Photovolt*. 2018;8:1023-1028.
66. Kanda H, Shibayama N, Uzum A, et al. Facile fabrication method of small-sized crystal silicon solar cells for ubiquitous applications and tandem device with perovskite solar cells. *Mater Today Energy*. 2018;7:190-198.
67. Choi IY, Kim CU, Park W, et al. Two-terminal mechanical perovskite/silicon tandem solar cells with transparent conductive adhesives. *Nano Energy*. 2019;65:104044.
68. Werner J, Weng C-H, Walter A, et al. Efficient monolithic perovskite/silicon tandem solar cell with cell area >1 cm2. *J Phys Chem Lett*. 2016;7:161-166.
69. Albrecht S, Saliba M, Correa Baena JP, et al. Monolithic perovskite/silicon-heterojunction tandem solar cells processed at low temperature. *Energ Environ Sci*. 2016;9:81-88.
70. Bush KA, Palmstrom AF, Yu ZJ, et al. 23.6%-efficient monolithic perovskite/silicon tandem solar cells with improved stability. *Nat Energy*. 2017;2:17009.
71. Fan R, Zhou N, Zhang L, et al. Toward full solution processed perovskite/Si monolithic tandem solar device with PCE exceeding 20%. *Sol RRL*. 2017;1:1700149.
72. Zhu S, Yao X, Ren Q, et al. Transparent electrode for monolithic perovskite/silicon-heterojunction two-terminal tandem solar cells. *Nano Energy*. 2018;45:280-286.
73. Qiu Z, Xu Z, Li N, et al. Monolithic perovskite/Si tandem solar cells exceeding 22% efficiency via optimizing top cell absorber. *Nano Energy*. 2018;53:798-807.
74. Sahli F, Kamino BA, Werner J, et al. Improved optics in monolithic perovskite/silicon tandem solar cells with a nanocrystalline silicon recombination junction. *Adv Energy Mater*. 2018;8:1701609.
75. Stannowski B, Mazzarella L, Lin Y, et al. Nanocrystalline silicon oxide interlayer in monolithic perovskite/silicon heterojunction tandem solar cells with total current density >39 mA/cm2. 2018 IEEE 7th World Conference on Photovoltaic Energy Conversion (WCPEC); 2018; 2627-2630. https://doi.org/10.1109/PVSC.2018.8547825.
76. Bush KA, Manzoor S, Frohna K, et al. Minimizing current and voltage losses to reach 25% efficient monolithic two-terminal perovskite–silicon tandem solar cells. *ACS Energy Lett*. 2018;3(9):2173-2180.
77. Sahli F, Werner J, Kamino BA, et al. Fully textured monolithic perovskite/silicon tandem solar cells with 25.2% power conversion efficiency. *Nat Mater*. 2018;17:820-826.
78. Jošt M, Köhnen E, Morales-Vilches AB, et al. Textured interfaces in monolithic perovskite/silicon tandem solar cells: advanced light management for improved efficiency and energy yield. *Energ Environ Sci*. 2018;11:3511-3523.
79. Hou F, Yan L, Shi B, et al. Monolithic perovskite/silicon-heterojunction tandem solar cells with open-circuit voltage of over 1.8 V. *ACS Appl Energy Mater*. 2019;2:243-249.
80. Hou F, Han C, Isabella O, et al. Inverted pyramidally-textured PDMS antireflective foils for perovskite/silicon tandem solar cells with flat top cell. *Nano Energy*. 2019;56:234-240.
81. Kamino BA, Paviet-Salomon B, Moon S-J, et al. Low-temperature screen-printed metallization for the scale-up of two-terminal perovskite–silicon tandems. *ACS Appl Energy Mater*. 2019;2:3815-3821.
82. Park IJ, Park JH, Ji SG, Park MA, Jang JH, Kim JY. A three-terminal monolithic perovskite/Si tandem solar cell characterization platform. *Joule*. 2019;3:807-818.
83. Nogay G, Sahli F, Werner J, et al. 25.1%-efficient monolithic perovskite/silicon tandem solar cell based on a p-type monocrystalline textured silicon wafer and high-temperature Passivating contacts. *ACS Energy Lett*. 2019;4:844-845.
84. Chen B, Yu Z, Liu K, et al. Grain engineering for perovskite/silicon monolithic tandem solar cells with efficiency of 25.4%. *Joule*. 2019;3:177-190.
85. Hou Y, Aydin E, De Bastiani M, et al. Efficient tandem solar cells with solution-processed perovskite on textured crystalline silicon. *Science*. 2020;367:1135-1140.
86. Xu J, Boyd CC, Yu ZJ, et al. Triple-halide wide–band gap perovskites with suppressed phase segregation for efficient tandems. *Science*. 2020;367:1097-1104.
87. Chen B, Yu ZJ, Manzoor S, et al. Blade-coated perovskites on textured silicon for 26%-efficient monolithic Perovskite/silicon tandem solar cells. *Joule*. 2020;4:850-864.
88. Kim D, Jung HJ, Park IJ, et al. Efficient, stable silicon tandem cells enabled by anion-engineered wide-bandgap perovskites. *Science*. 2020;368:155-160.
89. Ahn N, Son D-Y, Jang I-H, Kang SM, Choi M, Park NG. Highly reproducible perovskite solar cells with average efficiency of 18.3% and best efficiency of 19.7% fabricated via Lewis base adduct of lead(II) iodide. *J Am Chem Soc*. 2015; 137:8696-8699.
90. Whitaker JB, Kim DH, Larson BW, et al. Scalable slot-die coating of high performance perovskite solar cells. *Sustain Energy Fuels*. 2018;2:2442-2449.

91. Kim JH, Williams ST, Cho N, Chueh CC, Jen AKY. Enhanced environmental stability of planar heterojunction perovskite solar cells based on blade-coating. *Adv Energy Mater*. 2015;5:1401229.
92. Zuo C, Vak D, Angmo D, Ding L, Gao M. One-step roll-to-roll air processed high efficiency perovskite solar cells. *Nano Energy*. 2018;46:185-192.
93. Cotella G, Baker J, Worsley D, et al. One-step deposition by slot-die coating of mixed lead halide perovskite for photovoltaic applications. *Sol Energy Mater Sol Cells*. 2017;159:362-369.
94. Ulicna S, Dou B, Kim DH, et al. Scalable deposition of high-efficiency perovskite solar cells by spray-coating. *ACS Appl Energy Mater*. 2018;1:1853-1857.
95. Park M, Cho W, Lee G, et al. Highly reproducible large-area Perovskite solar cell fabrication via continuous Megasonic spray coating of CH3NH3PbI3. *Small*. 2019;15:1804005.
96. Giacomo FD, Shanmugam S, Fledderus H, et al. Up-scalable sheet-to-sheet production of high efficiency perovskite module and solar cells on 6-in. Substrate using slot die coating. *Sol Energy Mater Sol Cells*. 2018;181:53-59.
97. Deng Y, Van Brackle CH, Dai X, et al. Tailoring solvent coordination for high-speed, room-temperature blading of perovskite photovoltaic films. *Sci Adv*. 2019;5:eaax7537.
98. Liu M, Johnston MB, Snaith HJ. Efficient planar heterojunction perovskite solar cells by vapour deposition. *Nature*. 2013;501:395-398.
99. Zhao D, Ke W, Grice CR, et al. Annealing-free efficient vacuum-deposited planar perovskite solar cells with evaporated fullerenes as electron-selective layers. *Nano Energy*. 2016;19:88-97.
100. Ma Q, Huang S, Wen X, Green MA, Ho-Baillie AWY. Hole transport layer free inorganic CsPbIBr2 perovskite solar cell by dual source thermal evaporation. *Adv Energy Mater*. 2016;6:1502202.
101. Zheng Z-H, Lan H-B, Su Z-H, et al. Single source thermal evaporation of two-dimensional perovskite thin films for photovoltaic applications. *Sci Rep*. 2019;9:17422.
102. Lei T, Li F, Zhu X, et al. Flexible perovskite solar modules with functional layers fully vacuum deposited. *Sol RRL*. 2020;4:2000292.
103. Roß M, Gil-Escrig L, Al-Ashouri A, et al. Co-evaporated p-i-n perovskite solar cells beyond 20% efficiency: impact of substrate temperature and hole-transport layer. *ACS Appl Mater Interfaces*. 2020;12:39261-39272.
104. Li J, Wang H, Chin XY, et al. Highly efficient thermally co-evaporated perovskite solar cells and mini-modules. *Joule*. 2020;4:1035-1053.
105. Longo G, Gil-Escrig L, Degen MJ, Sessolo M, Bolink HJ. Perovskite solar cells prepared by flash evaporation. *Chem Com*. 2015;51:7376-7378.
106. Li G, Ho JYL, Wong M, Kwok HS. Low cost, high throughput and centimeter-scale fabrication of efficient hybrid perovskite solar cells by closed space vapor transport. *Phys Status Solidi RRL*. 2016;10:153-157.
107. Aitola K, Domanski K, Correa-Baena J-P, et al. High temperature-stable perovskite solar cell based on low-cost carbon nanotube hole contact. *Adv Mater*. 2017;29:1606398.
108. Kim Y, Jung EH, Kim G, Kim D, Kim BJ, Seo J. Sequentially fluorinated PTAA polymers for enhancing VOC of high-performance perovskite solar cells. *Adv Energy Mater*. 2018;8:1801668.
109. Zhou L, Chang J, Liu Z, et al. Enhanced planar perovskite solar cell efficiency and stability using a perovskite/PCBM heterojunction formed in one step. *Nanoscale*. 2018;10:3053-3059.
110. Abzieher T, Moghadamzadeh S, Schackmar F, et al. Electron-beam-evaporated nickel oxide hole transport layers for perovskite-based photovoltaics. *Adv Energy Mater*. 2019;9:1802995.
111. Yang IS, Sohn MR, Sung SD, et al. Formation of pristine CuSCN layer by spray deposition method for efficient perovskite solar cell with extended stability. *Nano Energy*. 2017;32:414-421.
112. Yun AJ, Kim J, Hwang T, Park B. Origins of efficient perovskite solar cells with low-temperature processed SnO2 electron transport layer. *ACS Appl Energy Mater*. 2019;2:3554-3560.
113. Feng J, Yang Z, Yang D, et al. E-beam evaporated Nb2O5 as an effective electron transport layer for large flexible perovskite solar cells. *Nano Energy*. 2017;36:1-8.
114. Zhai Y, Wang Z, Wang G, Peijnenburg WJGM, Vijver MG. The fate and toxicity of Pb-based perovskite nanoparticles on soil bacterial community: impacts of pH, humic acid, and divalent cations. *Chemosphere*. 2020;249:126564.
115. Zhang X, Wang W, Xu B, et al. Less-lead control toward highly efficient formamidinium-based perovskite light-emitting diodes. *ACS Appl Mater Interfaces*. 2018;10:24242-24248.
116. Soleimanioun N, Rani M, Sharma S, Kumar A, Tripathi SK. Binary metal zinc-lead perovskite built-in air ambient: towards lead-less and stable perovskite materials. *Sol Energy Mater Sol Cells*. 2019;191:339-344.
117. Shao S, Liu J, Portale G, et al. Highly reproducible Sn-based hybrid perovskite solar cells with 9% efficiency. *Adv Energy Mater*. 2018;8:1702019.
118. Chen S, Deng Y, Gu H, et al. Trapping lead in perovskite solar modules with abundant and low-cost cation-exchange resins. *Nat Energy*. 2020;5:1003-1011.
119. Zhao Z, Gu F, Rao H, et al. Metal halide perovskite materials for solar cells with long-term stability. *Adv Energy Mater*. 2019;9:1802671.
120. Yi C, Luo J, Meloni S, et al. Entropic stabilization of mixed A-cation ABX3 metal halide perovskites for high performance perovskite solar cells. *Energ Environ Sci*. 2016;9:656-662.
121. Noh JH, Im SH, Heo JH, Mandal TN, Seok SI. Chemical management for colorful, efficient, and stable inorganic–organic hybrid nanostructured solar cells. *Nano Lett*. 2013;13:1764-1769.
122. Grancini G, Roldán-Carmona C, Zimmermann I, et al. One-year stable perovskite solar cells by 2D/3D interface engineering. *Nat Comm*. 2017;8:15684.
123. Gharibzadeh S, Nejand AB, Jakoby M, et al. Record open-circuit voltage wide-bandgap perovskite solar cells utilizing 2D/3D perovskite heterostructure. *Adv Energy Mater*. 2019;9:1803699.
124. Chen P, Bai Y, Wang S, Lyu M, Yun JH, Wang L. In situ growth of 2D perovskite capping layer for stable and efficient perovskite solar cells. *Adv Funct Mater*. 2018;28:1706923.
125. Cheacharoen R, Boyd CC, Burkhard GF, et al. Encapsulating perovskite solar cells to withstand damp heat and thermal cycling. *Sustain Energy Fuels*. 2018;2:2398-2406.
126. Boyd CC, Cheacharoen R, Bush KA, Prasanna R, Leijtens T, McGehee MD. Barrier design to prevent metal-induced degradation and improve thermal stability in Perovskite solar cells. *ACS Energy Lett*. 2018;3:1772-1778.
127. Cheacharoen R, Bush KA, Rolston N, et al. Damp heat, temperature cycling and UV stress testing of encapsulated

perovskite photovoltaic cells. 2018 IEEE 7th World Conference on Photovoltaic Energy Conversion (WCPEC); 2018; 3489-3502. https://doi.org/10.1109/PVSC.2018.8547430.

128. Levrat J, Allebé C, Badel N, et al. High-performance heterojunction crystalline silicon photovoltaic technology. 2014 IEEE 40th Photovoltaic Specialist Conference (PVSC); 2014; 1218-1222. https://doi.org/10.1109/PVSC.2014.6925134.

AUTHOR BIOGRAPHIES

Hyesung Park is currently an Associate Professor in School of Energy and Chemical Engineering at Ulsan National Institute of Science and Technology (UNIST), South Korea. He received his MS and PhD degrees in Mechanical Engineering and Electrical Engineering and Computer Science from Massachusetts Institute of Technology (MIT) in 2007 and 2012. He was a postdoctoral associate at MIT from 2012 to 2013 and postdoctoral fellow at Northwestern University in 2014. His research interests focus on synthesis of low-dimensional materials such as graphene, transition metal dichalcogenides, and nanowires, and their applications into functional devices in nanoelectronics, nanophotonics, energy harvesting, and bioelectronics.

Myoung Hoon Song is a professor of the School of Materials Science and Engineering at UNIST, Republic of Korea (2009-present). He received his PhD (August 2005) from the Department of Organic and Polymeric Materials, the Tokyo Institute of Technology, Japan. He joined the Optoelectronic Group of the Cavendish Lab., University of Cambridge, United Kingdom as a Post-DOC (2007-2009). His main research fields are organic/polymeric materials and organic/metal-halide-perovskite-based optoelectronic devices.

Kyoung Jin Choi is Professor in School of Materials Science and Engineering, Ulsan National Institute of Science and Technology (UNIST). He received his PhD degree in Department of Materials Science and Engineering of Pohang University of Science and Technology (POSTEC), Korea in 2001. His recent research interest is focused on semiconductor nanowires, quantum dots, photoelectrochemical (PEC) water splitting based on visible-light photocatalysts, piezoelectric & thermoelectric energy harvester, and perovskite/silicon tandem solar cells.

SUPPORTING INFORMATION

Additional supporting information may be found online in the Supporting Information section at the end of this article.

How to cite this article: Kim CU, Jung ED, Noh YW, et al. Strategy for large-scale monolithic Perovskite/Silicon tandem solar cell: A review of recent progress. *EcoMat*. 2021;3:e12084. https://doi.org/10.1002/eom2.12084